

# New gravitational self-force analytical results for eccentric orbits around a Schwarzschild black hole

Donato Bini<sup>1</sup>, Thibault Damour<sup>2</sup>, and Andrea Geralico<sup>1</sup>

<sup>1</sup>*Istituto per le Applicazioni del Calcolo “M. Picone”, CNR, I-00185 Rome, Italy*

<sup>2</sup>*Institut des Hautes Etudes Scientifiques, 91440 Bures-sur-Yvette, France*

(Dated: May 4, 2016)

We raise the analytical knowledge of the eccentricity-expansion of the Detweiler-Barack-Sago redshift invariant in a Schwarzschild spacetime up to the 9.5th post-Newtonian order (included) for the  $e^2$  and  $e^4$  contributions, and up to the 4th post-Newtonian order for the higher eccentricity contributions through  $e^{20}$ . We convert this information into an analytical knowledge of the effective-one-body radial potentials  $\bar{d}(u)$ ,  $\rho(u)$  and  $q(u)$  through the 9.5th post-Newtonian order. We find that our analytical results are compatible with current corresponding numerical self-force data.

## I. INTRODUCTION

A fruitful *synergy* between various methods for approximating the general relativistic two-body problem has developed over the last years, with accelerated progress over the last months. The concerned approximation methods are: post-Newtonian (PN) theory, self-force (SF) theory, and numerical relativity (NR). The synergy between these approximation methods was greatly facilitated by the construction of theoretical *bridges* connecting the various methods. Among these bridges, two have been particularly useful: the effective-one-body (EOB) formalism [1–4], and the first law of binary mechanics [5–7]. Examples of synergies between PN and SF facilitated by EOB and/or the first law are Refs. [8–30].

This paper is a follow-up of Ref. [27]. It concerns the first self-force (1SF) conservative dynamics of the eccentric orbits of a small mass  $m_1$  around a (non-spinning) large mass  $m_2$  (described by a Schwarzschild black hole). Our results complete the results of both Ref. [27] and of the recent related Refs. [28, 29]. Before entering the details of our new results we summarize in Table I how our results go beyond present analytical knowledge in terms of the decomposition of the (gauge-invariant) 1SF contribution  $\delta U(p, e)$  to the Detweiler-Barack-Sago [31, 32] average redshift  $U(p, e)$  in powers of the eccentricity  $e$ , i.e.,  $\delta U(p, e) = \sum_n \delta U^{e^n}(u_p)e^n$ . [We use in the present paper the same notation as in Ref. [27]. In particular,  $u_p \equiv 1/p$  denotes the inverse semi-latus rectum of the considered eccentric orbit. In addition, we denote  $M \equiv m_1 + m_2$ ,  $\mu \equiv m_1 m_2 / (m_1 + m_2)$  and  $\nu \equiv \mu / M = m_1 m_2 / (m_1 + m_2)^2$  in our EOB considerations.]

Table I shows that our new results are of two different types. On the one hand, we improve the PN knowledge of the contributions to  $\delta U$  of order  $e^2$  and  $e^4$  to the 9.5PN level (previous analytical knowledge was the 6.5PN level for  $\delta U^{e^2}$  [27] and the 4PN one for  $\delta U^{e^4}$  [27, 33]). On the other hand, we combine the 4PN results of [33] with the eccentric first law [7] to compute the 4PN-accurate values of  $\delta U^{e^n}$  for the high values of  $n$ :  $n = 12, 14, 16, 18, 20$  (previous similar 4PN-level knowledge concerned  $n = 6, 8, 10$  [28]). [We also give below the 4PN knowledge of the corresponding high

TABLE I. Present analytical knowledge of  $\delta U^{e^n}$  along eccentric orbits in a Schwarzschild spacetime.

$n$	$\delta U^{e^n}$	Refs.
0	22.5PN	Kavanagh et al.[25]
2	9.5PN	This paper
4	9.5PN	This paper
6	4PN	Hopper et al.[28]
8	4PN	Hopper et al.[28]
10	4PN	Hopper et al.[28]
12	4PN	This paper
14	4PN	This paper
16	4PN	This paper
18	4PN	This paper
20	4PN	This paper

eccentricity powers of the alternative redshift function  $\delta z_1(p, e) = \sum_n \delta z_1^{e^n}(u_p)e^n$ , where  $z_1 = 1/U$ .]

To complete our results on the coefficients at orders  $e^2$  and  $e^4$  of the redshift function  $\delta U(p, e) = \sum_n \delta U^{e^n}(u_p)e^n$ , we shall also transcribe below our 9.5PN-accurate results in terms of the corresponding EOB potentials  $\bar{d}(u)$  and  $q(u) \equiv q_4(u)$ . [We also give the previously uncomputed 4PN values of the higher- $p_r$ -powers analogs of the  $O(p_r^4)$  EOB potential  $q(u) \equiv q_4(u)$ .]

Finally, we shall also explicitly compute the 9.5PN-accurate value of the gauge-invariant 1SF precession function  $\rho(u)$  defined in Ref. [8] and related there to the 1SF EOB potentials  $a(u)$  and  $\bar{d}(u)$ . The precession function  $\rho(u)$  is of particular interest because it can be directly extracted from SF numerical computations of the dynamics of slightly eccentric orbits [9] *without* making use of the eccentric first law. Therefore a comparison between our 9.5PN analytical computation of the precession function  $\rho(u)$  (which combines SF theory with the eccentric first law [7]) and of a purely dynamical SF numerical computation of the precession of eccentric orbits (as in [9]) would be a useful check of the assumptions underlying the theoretical bridges (EOB and the first law) used in connecting SF and PN results.

## II. NOVEL ANALYTICAL RESULTS FOR $\delta U^{e^2}$ AND $\delta U^{e^4}$ UP TO THE 9.5PN ORDER

Our new, 9.5PN-accurate, results for  $\delta U^{e^2}$  and  $\delta U^{e^4}$  have been obtained by following the approach of our previous papers [18, 27]. Let us only recall that our approach combines standard Regge-Wheeler-Zerilli first order perturbation theory with the Mano-Suzuki-Takasugi (MST) [34, 35] hypergeometric-expansion technique (here used up to the multipolar  $l = 7$  solution included). The main steps of this, by now, well established procedure are sketched in Appendix A.

We have raised the analytical knowledge of  $\delta U^{e^2}$  from

the 6.5PN level obtained in our previous work [27] up to the 9.5PN level. Note that the conversion between PN order and meaningful powers of  $u_p$ , or equivalently<sup>1</sup>  $u$  or  $x$ , depends on the considered SF or EOB function. More precisely, the  $n$ th PN order corresponds to: (1) a term  $\propto u^{n+1}$  in  $a(u)$  (and  $\delta U(u, e)$ ); (2) a term  $\propto u^n$  in  $\bar{d}(u)$  or  $\rho(u)$ ; and (3) a term  $\propto u^{n-1}$  in  $q(u)$ . Therefore, our current 9.5PN accuracy (obtained by using hypergeometric expansions up to the multipolar order  $l = 7$ ) corresponds to error terms:  $O_{\ln}(u_p^{11})$  in  $\delta U(u_p, e)$ ;  $O_{\ln}(u^{10})$  in  $\bar{d}(u)$  or  $\rho(u)$ ; and  $O_{\ln}(u^9)$  in  $q(u)$ , where  $O_{\ln}(u^q)$  denotes some  $O(u^q \ln u^p)$  with a non specified natural integer  $p \geq 1$ . Our result for  $\delta U^{e^2}$  reads

$$\begin{aligned}
\delta U^{e^2}(u_p) = & u_p + 4u_p^2 + 7u_p^3 + \left(-\frac{5}{3} - \frac{41}{32}\pi^2\right) u_p^4 \\
& + \left(-\frac{11141}{45} + \frac{29665}{3072}\pi^2 - \frac{296}{15}\ln(u_p) - \frac{592}{15}\gamma - \frac{1458}{5}\ln(3) + \frac{3248}{15}\ln(2)\right) u_p^5 \\
& + \left(-\frac{2238629}{1575} - \frac{73145}{1536}\pi^2 + \frac{8696}{105}\ln(u_p) - \frac{167696}{105}\ln(2) + \frac{17392}{105}\gamma + \frac{42282}{35}\ln(3)\right) u_p^6 \\
& - \frac{232618}{1575}\pi u_p^{13/2} \\
& + \left(\frac{2750367763}{198450} - \frac{9765625}{4536}\ln(5) + \frac{41285072}{2835}\ln(2) + \frac{5102288}{2835}\gamma - \frac{673353}{280}\ln(3) + \frac{2551144}{2835}\ln(u_p)\right. \\
& \left. + \frac{9735101}{262144}\pi^4 - \frac{13433142863}{3538944}\pi^2\right) u_p^7 \\
& + \frac{2687231}{4410}\pi u_p^{15/2} \\
& + \left[\frac{1040896}{1575}\ln(u_p)^2 + \left(\frac{4163584}{1575}\gamma - \frac{85422206699}{5457375} + \frac{936036}{175}\ln(3) - \frac{109568}{1575}\ln(2)\right)\ln(u_p)\right. \\
& + \frac{471677766820151}{1719073125} - \frac{171448137814}{5457375}\ln(2) - \frac{301990638447}{4312000}\ln(3) + \frac{1228515625}{57024}\ln(5) - \frac{170844413398}{5457375}\gamma \\
& + \frac{1872072}{175}\gamma\ln(3) - \frac{219136}{1575}\ln(2)\gamma + \frac{1872072}{175}\ln(2)\ln(3) + \frac{4163584}{1575}\gamma^2 - \frac{23854914937}{503316480}\pi^4 \\
& \left. + \frac{936036}{175}\ln(3)^2 - \frac{77824}{15}\zeta(3) - \frac{8655872}{1575}\ln(2)^2 - \frac{80420758955297}{2477260800}\pi^2\right] u_p^8 \\
& + \frac{66757650913}{26195400}\pi u_p^{17/2}
\end{aligned}$$

<sup>1</sup> The name we give to the arguments in the various EOB potentials considered here is arbitrary, because we are expanding the corresponding *functions* (e.g.  $u \rightarrow \bar{d}(u)$ ) in powers of their argument. The traditional EOB notation for the argument is  $u$ ,

but as the corresponding physical quantity  $u = GM/c^2 r_{\text{EOB}}$  is numerically equal, modulo a  $O(\nu)$  correction, both to  $u_p = 1/p$  and to the frequency parameter usually denoted  $x$ , one sometimes calls the argument  $u_p$  or  $x$ .

$$\begin{aligned}
& + \left[ -\frac{2994904}{1225} \ln(u_p)^2 + \left( -\frac{11979616}{1225} \gamma + \frac{618506181077}{99324225} - \frac{5165694}{175} \ln(3) + \frac{55690528}{2205} \ln(2) \right) \ln(u_p) \right. \\
& - \frac{2205806334400049687}{1720792198125} - \frac{46585620571706}{165540375} \ln(2) + \frac{2452189382919}{8008000} \ln(3) - \frac{3191857421875}{36324288} \ln(5) \\
& - \frac{678223072849}{46332000} \ln(7) + \frac{1272610164394}{99324225} \gamma - \frac{10331388}{175} \gamma \ln(3) + \frac{111381056}{2205} \ln(2) \gamma \\
& - \frac{10331388}{175} \ln(2) \ln(3) - \frac{11979616}{1225} \gamma^2 + \frac{389897083139633}{16106127360} \pi^4 \\
& \left. - \frac{5165694}{175} \ln(3)^2 + \frac{1020736}{105} \zeta(3) + \frac{1391778208}{11025} \ln(2)^2 - \frac{79965804866374541}{554906419200} \pi^2 \right] u_p^9 \\
& + \left( -\frac{3936830890988503}{59935075200} \pi + \frac{100155852}{6125} \pi \ln(3) - \frac{2250424}{675} \pi^3 + \frac{120397684}{23625} \pi \ln(u_p) + \frac{665599064}{165375} \pi \ln(2) \right. \\
& \left. + \frac{240795368}{23625} \pi \gamma \right) u_p^{19/2} \\
& + \left[ -\frac{91608512384}{9823275} \ln(u_p)^2 + \left( \frac{2694566979}{53900} \ln(3) + \frac{105972007312260412}{442489422375} + \frac{76708984375}{1571724} \ln(5) \right. \right. \\
& \left. - \frac{366434049536}{9823275} \gamma - \frac{2995825170944}{9823275} \ln(2) \right) \ln(u_p) - \frac{86555681446617433123159}{949139810994375} + \frac{2694566979}{53900} \ln(3)^2 \\
& + \frac{213354316911514424}{442489422375} \gamma + \frac{1656928811171577752}{442489422375} \ln(2) - \frac{995870224363383}{1079078000} \ln(3) - \frac{38345561821484375}{56638646064} \ln(5) \\
& + \frac{315073184}{2835} \zeta(3) + \frac{193778020814}{868725} \ln(7) - \frac{113425393373}{100663296} \pi^6 - \frac{3608718872135173}{5651824640} \pi^2 \\
& + \frac{16005605256259137079}{16492674416640} \pi^4 + \frac{76708984375}{1571724} \ln(5)^2 - \frac{366434049536}{9823275} \gamma^2 - \frac{5991650341888}{9823275} \ln(2) \gamma \\
& + \frac{76708984375}{785862} \ln(2) \ln(5) - \frac{239758989824}{218295} \ln(2)^2 + \frac{2694566979}{26950} \gamma \ln(3) + \frac{76708984375}{785862} \gamma \ln(5) \\
& \left. + \frac{2694566979}{26950} \ln(2) \ln(3) \right] u_p^{10} \\
& + \left( -\frac{28108289357}{1157625} \pi \ln(u_p) + \frac{369663722}{33075} \pi^3 - \frac{56216578714}{1157625} \pi \gamma + \frac{15720247936467024947}{114535928707200} \pi \right. \\
& \left. + \frac{9003848366}{231525} \pi \ln(2) - \frac{839692089}{8575} \pi \ln(3) \right) u_p^{21/2} + O_{\ln}(u_p^{11}). \tag{1}
\end{aligned}$$

The numerical values of the coefficients in the latter expansion read

$$\begin{aligned}
\delta U^{e^2}(u_p) & = u_p + 4u_p^2 + 7u_p^3 - 14.31209731u_p^4 + (-345.3178497 - 19.73333333 \ln(u_p))u_p^5 \\
& + (-1575.580014 + 82.81904762 \ln(u_p))u_p^6 - 463.9942859u_p^{13/2} \\
& + (-14960.48992 + 899.8744268 \ln(u_p))u_p^7 + 1914.327703u_p^{15/2} \\
& + (-119420.1688 - 8298.710150 \ln(u_p) + 660.8863492 \ln(u_p)^2)u_p^8 + 8006.189854u_p^{17/2} \\
& + (-395945.586 - 14340.26852 \ln(u_p) - 2444.819592 \ln(u_p)^2)u_p^9 \\
& + (-226044.9538 + 16010.17903 \ln(u_p))u_p^{19/2} \\
& + (140039.6684 \ln(u_p) - 9325.658946 \ln(u_p)^2 - 2966833.394)u_p^{10} \\
& + (-76281.00237 \ln(u_p) + 436383.4353)u_p^{21/2} + O_{\ln}(u_p^{11}). \tag{2}
\end{aligned}$$

Similarly, we have extended the analytical knowledge of  $\delta U^{e^4}$  from 4PN (as obtained in our previous work [27]) up

to 9.5PN, namely

$$\begin{aligned}
\delta U^{e^4}(u_p) = & -2u_p^2 + \frac{1}{4}u_p^3 + \left(\frac{705}{8} - \frac{123}{256}\pi^2\right)u_p^4 \\
& + \left(\frac{247931}{360} - \frac{89395}{6144}\pi^2 + \frac{28431}{10}\ln(3) + \frac{292}{3}\gamma - \frac{64652}{15}\ln(2) + \frac{146}{3}\ln(u_p)\right)u_p^5 \\
& + \left(\frac{293423}{4200} - \frac{25493859}{2240}\ln(3) - \frac{601}{5}\ln(u_p) - \frac{1202}{5}\gamma + \frac{248378}{7}\ln(2) - \frac{9765625}{1344}\ln(5) + \frac{275167}{1024}\pi^2\right)u_p^6 \\
& + \frac{430889}{3150}\pi u_p^{13/2} \\
& + \left(-\frac{4815135047}{396900} - \frac{194385796}{945}\ln(2) - \frac{2260629}{320}\ln(3) + \frac{3470703125}{36288}\ln(5) - \frac{794596}{945}\gamma - \frac{397298}{945}\ln(u_p)\right. \\
& \left. - \frac{58818333}{1048576}\pi^4 + \frac{16293066631}{4718592}\pi^2\right)u_p^7 \\
& + \frac{13695499}{47040}\pi u_p^{15/2} \\
& + \left[\frac{497764}{1575}\ln(u_p)^2 + \left(\frac{1991056}{1575}\gamma - \frac{66544956203}{3969000} - \frac{11934459}{175}\ln(3) + \frac{195652496}{1575}\ln(2)\right)\ln(u_p)\right. \\
& + \frac{2047686486671407}{13752585000} - \frac{197388844553}{269500}\ln(2) + \frac{359853720161877}{275968000}\ln(3) - \frac{4691575390625}{8515584}\ln(5) \\
& - \frac{678223072849}{6082560}\ln(7) - \frac{66544956203}{1984500}\gamma - \frac{23868918}{175}\gamma\ln(3) + \frac{391304992}{1575}\ln(2)\gamma \\
& - \frac{23868918}{175}\ln(2)\ln(3) + \frac{1991056}{1575}\gamma^2 + \frac{924796757543}{2013265920}\pi^4 \\
& \left. - \frac{11934459}{175}\ln(3)^2 - \frac{37216}{15}\zeta(3) + \frac{751271824}{1575}\ln(2)^2 + \frac{27703501682741}{19818086400}\pi^2\right]u_p^8 \\
& + \frac{1023562537}{1552320}\pi u_p^{17/2} \\
& + \left[-\frac{10161819}{1225}\ln(u_p)^2\right. \\
& + \left(\frac{15523629993}{39200}\ln(3) + \frac{46249898026747}{305613000} - \frac{14486589644}{11025}\ln(2) - \frac{40647276}{1225}\gamma + \frac{3173828125}{14112}\ln(5)\right)\ln(u_p) \\
& + \frac{46285104644347}{152806500}\gamma - \frac{2067345910491191}{85899345920}\pi^4 + \frac{17923252135149887}{1986484500}\ln(2) - \frac{148748447195686881}{25113088000}\ln(3) \\
& - \frac{27786921439609375}{16273281024}\ln(5) + \frac{421370306260043}{219648000}\ln(7) + \frac{1655592}{35}\zeta(3) + \frac{4816187291152031551}{1529593065000} \\
& + \frac{3173828125}{14112}\ln(5)^2 - \frac{6286441324}{1225}\ln(2)^2 + \frac{3173828125}{7056}\gamma\ln(5) - \frac{40647276}{1225}\gamma^2 \\
& + \frac{15523629993}{39200}\ln(3)^2 - \frac{1712225112134041}{34681651200}\pi^2 + \frac{15523629993}{19600}\gamma\ln(3) - \frac{28973179288}{1025}\ln(2)\gamma \\
& \left. + \frac{3173828125}{7056}\ln(2)\ln(5) + \frac{15523629993}{19600}\ln(2)\ln(3)\right]u_p^9 \\
& + \left(-\frac{137457732402576571}{610248038400}\pi - \frac{40118366}{4725}\pi^3 + \frac{4292665162}{165375}\pi\gamma + \frac{2146332581}{165375}\pi\ln(u_p) + \frac{83149713482}{165375}\pi\ln(2)\right. \\
& \left. - \frac{1427220891}{6125}\pi\ln(3)\right)u_p^{19/2}
\end{aligned}$$

$$\begin{aligned}
& + \left[ -\frac{2438262007}{198450} \ln(u_p)^2 + \left( \frac{487959613018}{72765} \ln(2) + \frac{4899895367447}{4584195} + \frac{114443682651}{431200} \ln(3) - \frac{4876524014}{99225} \gamma \right. \right. \\
& - \left. \frac{40750244140625}{12573792} \ln(5) \right) \ln(u_p) - \frac{20377781024735400904328}{201332687180625} + \frac{9826562433694}{4584195} \gamma \\
& - \frac{176771772306908307}{276243968000} \ln(3) - \frac{40750244140625}{12573792} \ln(5)^2 - \frac{4876524014}{99225} \gamma^2 + \frac{114443682651}{431200} \ln(3)^2 \\
& + \frac{36307823919194}{1403325} \ln(2)^2 + \frac{536631960411}{215600} \ln(2) \ln(3) + \frac{114443682651}{215600} \gamma \ln(3) + \frac{19871612}{63} \zeta(3) \\
& - \frac{131229423889414613}{8895744000} \ln(7) - \frac{40750244140625}{6286896} \gamma \ln(5) + \frac{1167313947555}{268435456} \pi^6 + \frac{975919226036}{72765} \ln(2) \gamma \\
& + \frac{628897515069490765625}{14499493392384} \ln(5) - \frac{707217483022033957}{1109812838400} \pi^2 - \frac{40750244140625}{6286896} \ln(2) \ln(5) \\
& + \left. \frac{10992948747002026551}{10995116277760} \pi^4 - \frac{476838331512979466}{9833098275} \ln(2) \right] u_p^{10} \\
& + \left( \frac{16759623823}{176400} \pi^3 + \frac{80294969715785936774437}{45814371482880000} \pi - \frac{6503164207213}{37044000} \pi \ln(u_p) - \frac{100110344015981}{18522000} \pi \ln(2) \right. \\
& + \left. \frac{2087606910177}{1372000} \pi \ln(3) - \frac{6503164207213}{18522000} \pi \gamma + \frac{206298828125}{296352} \pi \ln(5) \right) u_p^{21/2} + O_{\ln}(u_p^{11}). \tag{3}
\end{aligned}$$

The numerical form of this expansion reads

$$\begin{aligned}
\delta U^{e^4}(u_p) = & -2.0u_p^2 + 0.25u_p^3 + 83.38296351u_p^4 + (737.1849552 + 48.66666667 \ln(u_p))u_p^5 \\
& + (2980.049710 - 120.2 \ln(u_p))u_p^6 + 429.7389577u_p^{13/2} \\
& + (19588.97635 - 420.4211640 \ln(u_p))u_p^7 + 914.6615445u_p^{15/2} \\
& + (62630.23815 - 4853.06274 \ln(u_p) + 316.0406349 \ln(u_p)^2)u_p^8 + 2071.490767u_p^{17/2} \\
& + (18432.5611 \ln(u_p) - 8295.362449 \ln(u_p)^2 + 837868.8305)u_p^9 \\
& + (-633183.2616 + 40773.40995 \ln(u_p))u_p^{19/2} \\
& + (764293.4202 \ln(u_p) - 12286.53065 \ln(u_p)^2 + 1154095.188)u_p^{10} \\
& + (4816799.276 - 551514.2235 \ln(u_p))u_p^{21/2} + O_{\ln}(u_p^{11}). \tag{4}
\end{aligned}$$

Using the relations explicitly written down in [7] we converted the new information on  $\delta U^{e^2}$  and  $\delta U^{e^4}$  into a

correspondingly improved knowledge of the EOB potentials  $\bar{d}(x)$  and  $q(x)$ , namely

$$\begin{aligned}
\bar{d}(x) = & 6x^2 + 52x^3 + \left( \frac{1184}{15}\gamma - \frac{6496}{15}\ln(2) + \frac{2916}{5}\ln(3) - \frac{23761}{1536}\pi^2 - \frac{533}{45} + \frac{592}{15}\ln(x) \right) x^4 \\
& + \left( -\frac{2840}{7}\gamma + \frac{120648}{35}\ln(2) - \frac{19683}{7}\ln(3) - \frac{63707}{512}\pi^2 + \frac{294464}{175} - \frac{1420}{7}\ln(x) \right) x^5 \\
& + \frac{264932}{1575}\pi x^{11/2} \\
& + \left( -\frac{64096}{45}\gamma - \frac{6381680}{189}\ln(2) + \frac{1765881}{140}\ln(3) + \frac{9765625}{2268}\ln(5) + \frac{135909}{262144}\pi^4 + \frac{229504763}{98304}\pi^2 \right. \\
& \left. - \frac{31721400523}{2116800} - \frac{32048}{45}\ln(x) \right) x^6 \\
& - \frac{21288791}{17640}\pi x^{13/2} \\
& + \left( \frac{4187061434}{99225}\gamma - \frac{876544}{315}\ln(x)\gamma + \frac{8108032}{1575}\ln(2)\ln(x) + \frac{16216064}{1575}\ln(2)\gamma - \frac{3744144}{175}\ln(2)\ln(3) \right. \\
& - \frac{3744144}{175}\gamma\ln(3) + \frac{18024943666}{496125}\ln(2) + \frac{282753093897}{2156000}\ln(3) + \frac{16384}{3}\zeta(3) - \frac{3091796875}{66528}\ln(5) \\
& + \frac{33089536}{1575}\ln(2)^2 + \frac{31596265477}{251658240}\pi^4 + \frac{3755930660113}{247726080}\pi^2 - \frac{876544}{315}\gamma^2 - \frac{1872072}{175}\ln(3)^2 \\
& + \frac{629856}{55}\ln(6) - \frac{1340870864165051}{5501034000} - \frac{219136}{315}\ln(x)^2 - \frac{1872072}{175}\ln(3)\ln(x) + \frac{2093530717}{99225}\ln(x) \left. \right) x^7 \\
& - \frac{1173441809}{3492720}\pi x^{15/2} \\
& + \left( -\frac{281972594008247}{1986484500}\gamma + \frac{232751488}{11025}\ln(x)\gamma - \frac{31370368}{525}\ln(2)\ln(x) - \frac{62740736}{525}\ln(2)\gamma \right. \\
& + \frac{174802536}{1225}\ln(2)\ln(3) + \frac{174802536}{1225}\gamma\ln(3) + \frac{107340333276983}{283783500}\ln(2) - \frac{25726492389393}{49049000}\ln(3) \\
& - \frac{1096192}{35}\zeta(3) + \frac{1556814453125}{6054048}\ln(5) + \frac{678223072849}{23166000}\ln(7) - \frac{624682112}{2205}\ln(2)^2 + \frac{16273379175661}{1073741824}\pi^4 \\
& + \frac{2692389474594437}{92484403200}\pi^2 + \frac{232751488}{11025}\gamma^2 + \frac{87401268}{1225}\ln(3)^2 - \frac{2751525936}{17875}\ln(6) + \frac{58187872}{11025}\ln(x)^2 \\
& + \frac{87401268}{1225}\ln(3)\ln(x) - \frac{831440592970385544103}{440522802720000} - \frac{281464053976247}{3972969000}\ln(x) \left. \right) x^8 \\
& + \left( \frac{144712674728544827}{1678182105600}\pi - \frac{186756088}{33075}\pi\ln(x) + \frac{239421488}{23625}\ln(2)\pi + \frac{3490768}{945}\pi^3 - \frac{373512176}{33075}\pi\gamma \right. \\
& \left. - \frac{200311704}{6125}\pi\ln(3) \right) x^{17/2} \\
& + \left[ -\frac{145060456}{363825}\ln(x)^2 + \left( -\frac{4109882910365899}{19423404000} + \frac{2205013489376}{3274425}\ln(2) - \frac{580241824}{363825}\gamma - \frac{215213193}{770}\ln(3) \right. \right. \\
& \left. \left. - \frac{76708984375}{785862}\ln(5) \right) \ln(x) + \frac{8869707677468340294172589}{188984282366880000} - \frac{4125670253137099}{9711702000}\gamma \right. \\
& - \frac{23620001432239865033}{2359943586000}\ln(2) + \frac{18387195312716343}{4932928000}\ln(3) + \frac{1763600530764453125}{1812436674048}\ln(5) - \frac{215213193}{385}\gamma\ln(3) \\
& + \frac{117281890332}{125125}\ln(6) - \frac{7435264}{105}\zeta(3) - \frac{43503165672743}{92664000}\ln(7) + \frac{13438960917574667}{406931374080}\pi^2 - \frac{441262176956397691}{1030792151040}\pi^4 \\
& - \frac{215213193}{770}\ln(3)^2 - \frac{580241824}{363825}\gamma^2 + \frac{5132203667744}{1964655}\ln(2)^2 - \frac{76708984375}{785862}\ln(5)^2 - \frac{150232915593}{33544432}\pi^6 \\
& \left. \left. - \frac{76708984375}{392931}\gamma\ln(5) - \frac{215213193}{385}\ln(2)\ln(3) + \frac{4410026978752}{3274425}\ln(2)\gamma - \frac{76708984375}{392931}\ln(2)\ln(5) \right] x^9 \right. \\
& + \left( -\frac{10310051408772977303753}{22907185741440000}\pi - \frac{1836704419}{66150}\pi^3 + \frac{232145783843}{2315250}\pi\gamma - \frac{83839907743}{771750}\pi\ln(2) \right. \\
& \left. + \frac{39949476291}{171500}\pi\ln(3) + \frac{232145783843}{4630500}\pi\ln(x) \right) x^{19/2} + O_{\ln}(x^{10}) \tag{5}
\end{aligned}$$

and

$$\begin{aligned}
q(x) = & 8x^2 + \left( \frac{496256}{45} \ln(2) - \frac{33048}{5} \ln(3) - \frac{5308}{15} \right) x^3 \\
& + \left( \frac{10856}{105} \gamma - \frac{40979464}{315} \ln(2) + \frac{14203593}{280} \ln(3) + \frac{9765625}{504} \ln(5) - \frac{93031}{1536} \pi^2 + \frac{1295219}{350} + \frac{5428}{105} \ln(x) \right) x^4 \\
& + \frac{88703}{1890} \pi x^{9/2} \\
& + \left( -\frac{617716}{315} \gamma - \frac{308858}{315} \ln(x) + \frac{65887036}{63} \ln(2) - \frac{36073593}{112} \ln(3) - \frac{8787109375}{27216} \ln(5) + \frac{81030481}{65536} \pi^2 \right. \\
& \left. + \frac{559872}{7} \ln(6) - \frac{7518451741}{1270080} \right) x^5 \\
& - \frac{714117331}{846720} \pi x^{11/2} \\
& + \left( \frac{138169844888}{1819125} \gamma + \frac{69084922444}{1819125} \ln(x) - \frac{3250526464}{4725} \ln(2) \gamma + \frac{13728528}{35} \ln(2) \ln(3) + \frac{13728528}{35} \gamma \ln(3) \right. \\
& - \frac{527856862616}{16372125} \ln(2) - \frac{12960490645107}{6899200} \ln(3) + \frac{25344}{5} \zeta(3) + \frac{27397616796875}{9580032} \ln(5) + \frac{678223072849}{2280960} \ln(7) \\
& - \frac{2065918336}{1575} \ln(2)^2 - \frac{109837713789}{83886080} \pi^4 + \frac{1463044337673}{91750400} \pi^2 - \frac{451968}{175} \gamma^2 + \frac{6864264}{35} \ln(3)^2 - \frac{579887424}{385} \ln(6) \\
& \left. - \frac{451968}{175} \ln(x) \gamma + \frac{6864264}{35} \ln(3) \ln(x) - \frac{939101654498857}{3056130000} - \frac{112992}{175} \ln(x)^2 - \frac{1625263232}{4725} \ln(2) \ln(x) \right) x^6 \\
& + \frac{226615901761}{167650560} \pi x^{13/2} \\
& + \left( -\frac{29186389360543}{36786750} \gamma - \frac{3173828125}{2646} \ln(2) \ln(5) - \frac{3173828125}{2646} \gamma \ln(5) - \frac{9440966259}{4900} \ln(3) \ln(x) \right. \\
& + \frac{322866894016}{33075} \ln(2) \gamma - \frac{9440966259}{2450} \ln(2) \ln(3) - \frac{9440966259}{2450} \gamma \ln(3) - \frac{97783791533166503}{2979726750} \ln(2) \\
& + \frac{87139874452615209}{6278272000} \ln(3) - \frac{2452928}{35} \zeta(3) - \frac{2899973891640625}{452035584} \ln(5) - \frac{9257841833399257}{1482624000} \ln(7) \\
& + \frac{210393017888}{11025} \ln(2)^2 + \frac{19047555410493}{10737418240} \pi^4 - \frac{3975430726567129}{92484403200} \pi^2 + \frac{168910688}{3675} \gamma^2 - \frac{9440966259}{4900} \ln(3)^2 \\
& + \frac{2573147182608}{175175} \ln(6) - \frac{3173828125}{5292} \ln(5)^2 - \frac{3173828125}{5292} \ln(5) \ln(x) + \frac{161433447008}{33075} \ln(2) \ln(x) \\
& \left. + \frac{690294961714478265797}{293681868480000} - \frac{29186389360543}{73573500} \ln(x) + \frac{42227672}{3675} \ln(x)^2 + \frac{168910688}{3675} \ln(x) \gamma \right) x^7 \\
& + \left( \frac{8192870254937920639}{30981823488000} \pi - \frac{15200768606}{11025} \ln(2) \pi - \frac{11631519958}{496125} \pi \gamma + \frac{4598822871}{6125} \pi \ln(3) + \frac{108705794}{14175} \pi^3 \right. \\
& \left. - \frac{5815759979}{496125} \pi \ln(x) \right) x^{15/2} \\
& + \left[ \frac{131228022231920707}{196661965500} \gamma + \frac{23800697662770506993}{65553988500} \ln(2) - \frac{4958146688407013943}{39463424000} \ln(3) \right. \\
& - \frac{4492372832662738703125}{43498480177152} \ln(5) - \frac{2906254027437804}{67442375} \ln(6) + \frac{1519264}{315} \zeta(3) + \frac{710656240002840019}{10674892800} \ln(7) \\
& + \frac{472332484052074531}{678218956800} \pi^2 + \frac{9617337404302759049}{24739011624960} \pi^4 + \frac{105898193359375}{9430344} \ln(5)^2 + \frac{226550022075}{33554432} \pi^6 \\
& - \frac{188687137328}{1091475} \gamma^2 - \frac{7036471296}{2695} \ln(6)^2 + \frac{181114018983}{15400} \ln(3)^2 - \frac{4527732156900112}{29469825} \ln(2)^2 \\
& - \frac{85388056818784}{1091475} \ln(2) \gamma - \frac{14072942592}{2695} \ln(2) \ln(6) + \frac{105898193359375}{4715172} \gamma \ln(5) - \frac{14072942592}{2695} \gamma \ln(6) \\
& + \frac{181114018983}{7700} \gamma \ln(3) + \frac{105898193359375}{4715172} \ln(2) \ln(5) + \frac{181114018983}{7700} \ln(2) \ln(3) - \frac{7190610346934768219939609}{161986527743040000} \\
& + \left( -\frac{7036471296}{2695} \ln(6) + \frac{105898193359375}{9430344} \ln(5) + \frac{131815385968880707}{39323931000} - \frac{188687137328}{1091475} \gamma + \frac{181114018983}{15400} \ln(3) \right. \\
& \left. - \frac{42694028409392}{1091475} \ln(2) \right) \ln(x) - \frac{47171784332}{1091475} \ln(x)^2 \Big] x^8
\end{aligned}$$

$$\begin{aligned}
& + \left( -\frac{309249455540719514934031}{84580378122240000}\pi - \frac{206298828125}{111132}\pi \ln(5) - \frac{431496991403}{3175200}\pi^3 + \frac{52009951116491}{111132000}\pi\gamma \right. \\
& \left. + \frac{88244053021571}{4445280}\pi \ln(2) - \frac{21764539709991}{2744000}\pi \ln(3) + \frac{52009951116491}{222264000}\pi \ln(x) \right) x^{17/2} + O_{\ln}(x^9). \quad (6)
\end{aligned}$$

As mentioned above, another useful dynamical function is the precession function  $\rho(u)$  introduced in [8] and related there to the EOB potentials  $a(u)$  and  $\bar{d}(u)$ . Namely (denoting the argument of the function  $\rho$  as  $x$ )

$$\rho(x) = \rho_E(x) + \rho_a(x) + \rho_{\bar{d}}(x), \quad (7)$$

with

$$\begin{aligned}
\rho_E(x) &= 4x \left( 1 - \frac{1-2x}{\sqrt{1-3x}} \right), \\
\rho_a(x) &= a(x) + xa'(x) + \frac{1}{2}x(1-2x)a''(x), \\
\rho_{\bar{d}}(x) &= (1-6x)\bar{d}(x). \quad (8)
\end{aligned}$$

We then find

$$\begin{aligned}
\rho(x) &= 14x^2 + \left( \frac{397}{2} - \frac{123}{16}\pi^2 \right) x^3 + \left( \frac{5024}{15}\gamma - \frac{215729}{180} + \frac{2512}{15}\ln(x) + \frac{2916}{5}\ln(3) + \frac{1184}{15}\ln(2) + \frac{58265}{1536}\pi^2 \right) x^4 \\
&+ \left( \frac{27824}{35}\ln(2) - \frac{6325051}{800} + \frac{1135765}{1024}\pi^2 - \frac{202662}{35}\ln(3) - \frac{22672}{7}\gamma - \frac{11336}{7}\ln(x) \right) x^5 \\
&+ \frac{199876}{315}\pi x^{11/2} \\
&+ \left( \frac{4990303259}{589824}\pi^2 - \frac{256727518799}{6350400} + \frac{435213}{20}\ln(3) + \frac{3606884}{945}\gamma - \frac{37648124}{945}\ln(2) + \frac{1803442}{945}\ln(x) \right. \\
&\left. - \frac{7335303}{32768}\pi^4 + \frac{9765625}{2268}\ln(5) \right) x^6 \\
&- \frac{1429274}{225}\pi x^{13/2} \\
&+ \left( -\frac{3725312}{1575}\ln(2)^2 - \frac{419921875}{6048}\ln(5) - \frac{3744144}{175}\gamma \ln(3) - \frac{3744144}{175}\ln(2)\ln(3) + \frac{253952}{15}\zeta(3) \right. \\
&- \frac{13586432}{1575}\ln(x)\gamma - \frac{230019793907682883}{440082720000} - \frac{1872072}{175}\ln(3)\ln(x) - \frac{20598784}{1575}\ln(2)\gamma + \frac{12659060941523}{1238630400}\pi^2 \\
&+ \frac{681396625634}{5457375}\gamma + \frac{229716339147}{2156000}\ln(3) - \frac{3396608}{1575}\ln(x)^2 + \frac{1823766172754}{5457375}\ln(2) - \frac{10299392}{1575}\ln(2)\ln(x) \\
&+ \frac{471044952937}{251658240}\pi^4 + \frac{340698312817}{5457375}\ln(x) - \frac{1872072}{175}\ln(3)^2 - \frac{13586432}{1575}\gamma^2 \left. \right) x^7 \\
&+ \frac{18719967989}{1455300}\pi x^{15/2} \\
&+ \left( -\frac{82814168955181}{132432300}\ln(2) + \frac{36686848}{441}\ln(x)\gamma + \frac{1920044921875}{4036032}\ln(5) + \frac{2269129471514627499419}{176209121088000} \right. \\
&+ \frac{148969692}{1225}\ln(3)^2 + \frac{36686848}{441}\gamma^2 + \frac{103653376}{3675}\ln(2)\gamma + \frac{9171712}{441}\ln(x)^2 + \frac{297939384}{1225}\gamma \ln(3) \\
&- \frac{948480}{7}\zeta(3) + \frac{297939384}{1225}\ln(2)\ln(3) + \frac{678223072849}{23166000}\ln(7) + \frac{148969692}{1225}\ln(3)\ln(x) \\
&+ \frac{51826688}{3675}\ln(2)\ln(x) - \frac{6517218707007553}{55490641920}\pi^2 - \frac{1442495323220011}{3972969000}\ln(x) \\
&\left. - \frac{557542163367261}{392392000}\ln(3) - \frac{1444834607367211}{1986484500}\gamma - \frac{2049476608}{11025}\ln(2)^2 - \frac{626168320805261}{5368709120}\pi^4 \right) x^8
\end{aligned}$$



$$\begin{aligned}
& + \left( \frac{105699126344597143}{524431908000} \pi - \frac{4707645616}{165375} \pi \gamma - \frac{200311704}{6125} \pi \ln(3) - \frac{4004219056}{165375} \ln(2) \pi - \frac{2353822808}{165375} \pi \ln(x) \right. \\
& + \left. \frac{43996688}{4725} \pi^3 \right) x^{17/2} \\
& + \left[ -\frac{42935456848}{1091475} \ln(x)^2 + \left( -\frac{1995219783}{3850} \ln(3) - \frac{20475902395612297}{262215954000} - \frac{171741827392}{1091475} \gamma + \frac{2444046775616}{3274425} \ln(2) \right. \right. \\
& - \left. \left. \frac{76708984375}{785862} \ln(5) \right) \ln(x) - \frac{20657146063017097}{131107977000} \gamma + \frac{10969454340865467}{2466464000} \ln(3) + \frac{226626361596}{125125} \ln(6) \right. \\
& - \frac{76708984375}{785862} \ln(5)^2 - \frac{171741827392}{1091475} \gamma^2 - \frac{1995219783}{3850} \ln(3)^2 + \frac{6754948737728}{1964655} \ln(2)^2 \\
& - \frac{1995219783}{1925} \gamma \ln(3) - \frac{76708984375}{392931} \gamma \ln(5) + \frac{3956569170916362731724487183}{18142491107220480000} + \frac{8519104}{315} \zeta(3) \\
& - \frac{29163592132507}{46332000} \ln(7) - \frac{76708984375}{392931} \ln(2) \ln(5) + \frac{4888093551232}{3274425} \ln(2) \gamma - \frac{64674832921484375}{906218337024} \ln(5) \\
& + \frac{3466357618648439}{27128758272} \pi^2 + \frac{128148402261}{16777216} \pi^6 - \frac{1995219783}{1925} \ln(2) \ln(3) - \frac{6269062781928031361}{2748779069440} \pi^4 \\
& - \left. \frac{2702219779688690213}{235994358600} \ln(2) \right] x^9 \\
& + \left( \frac{174754006268}{1157625} \pi \ln(x) - \frac{2849519528}{33075} \pi^3 + \frac{349508012536}{1157625} \pi \gamma \right. \\
& + \left. \frac{16864298172}{42875} \pi \ln(3) - \frac{2195209992943672765961}{1431699108840000} \pi + \frac{51802382504}{385875} \pi \ln(2) \right) x^{19/2} + O_{\ln}(x^{10}). \tag{9}
\end{aligned}$$

### III. ESTIMATING THE ORDER OF MAGNITUDE OF THE COEFFICIENTS OF PN EXPANSIONS

Before comparing the numerical values of these 9.5PN-accurate functions to corresponding published numerical SF estimates [9, 29], it is useful to have at hand a rough estimate of the theoretical error associated with such PN-expanded functions. We shall do this via two complementary approaches. Our first estimate will follow the spirit of Section IV in Ref. [21]. The idea there was to use the existence of a power-law singularity at the lightring [12] of the various SF or EOB potentials to estimate, for a given potential  $f(u) = \sum_{n < N} f_n u^n + \epsilon_f^N(u)$ , both the order of magnitude of the PN expansion coefficients  $f_n$ , and that of the Nth PN remainder  $\epsilon_f^N(u) = O_f(u^N)$ , from the knowledge of its lightring singularity. The coarsest such estimate consists in saying that the radius of convergence of a power series<sup>2</sup>,  $\sum_N f_N u^N$ , is determined by the location of the singularity closest to the origin in the complex  $u$  plane. Assuming that the closest singularity is the lightring one at  $u = 1/3$  determines the radius of convergence as being  $|u|_{\text{conv}} = \frac{1}{3}$ . This simple consider-

ation tells us that the large- $N$  asymptotic values of the Taylor expansion coefficients  $f_N$  is of order

$$f_N \sim 3^N. \tag{10}$$

One can, however, refine this exponential estimate by power-law corrections in  $N$ . Indeed, given a certain function  $f(u) = \sum_N f_N u^N$ , its first derivative with respect to (wrt)  $u$  will be  $f'(u) = \sum_N N f_N u^{N-1}$ , so that  $(f')_N = (N+1)f_{N+1}$ . In other words, each derivative adds an asymptotic factor  $N$  to the growth of the  $f_N$ 's. For instance, the existence in EOB theory of the link (7), (8) between the precession function  $\rho(u)$  and the first two derivatives of the primary EOB radial (1SF) potential  $a(u)$  suggests that, asymptotically,

$$\rho_N \sim N^2 a_N, \tag{11}$$

where  $a_N$  are the PN expansion coefficients of  $a(u)$  and  $\rho_N$  those of  $\rho(u)$ . [Here, we assume that the PN coefficients  $\bar{d}_N$  of  $\bar{d}(u)$  do not cancel the growth with  $N$  entailed by the two derivatives in the first equation (8). Our numerical studies below will confirm this assumption.]

There is an alternative perspective on the additional power-law growth (of the type of the factor  $N^2$  in (11)). It consists in using more information about the singularity structure of the considered function  $f(u)$  near its closest singularity. Indeed, if we knew, for instance, that  $f(u)$  had a power-law singularity near  $u = \frac{1}{3}$  of the type

$$f^{\text{sing}}(u) = K_f (1 - 3u)^{-n_f}, \tag{12}$$

<sup>2</sup> Here, we formally proceed as if the PN expansion contained only integer powers. The existence of logarithmic corrections, starting at 4PN [8, 36], and of a sub-series, starting at 5.5PN [13, 14, 37], containing half-integer powers, indicates that, from a theoretical point of view, a more subtle treatment should be applied. See below for the logarithmic corrections.

( $K_f$  denoting a constant), we would expect<sup>3</sup> the expansion coefficients  $f_N$  of  $f(u)$  to be asymptotically approximated by the expansion coefficients of its singular piece (12), namely

$$f_N^{\text{sing}} = K_f \binom{-n_f}{N} 3^N \approx C_f N^{n_f-1} 3^N, \quad (13)$$

with  $C_f = K_f/\Gamma(n_f)$ . Here we see that while the location of the singularity determines the exponentially growing factor  $3^N$ , the sub-leading power-law growth  $\propto N^{n_f-1}$  would be determined by the power  $-n_f$  of the singular piece (12). Consistently with our remarks above, note that acting on  $f(u)$  by  $k$  derivatives changes  $n_f$  into  $n_f + k$ , and correspondingly increases the power-law growth of the  $f_N$ 's by  $+k$ .

Ref. [12] has found that the lightring singularity structure of the basic 1SF EOB potential  $a(u)$  was  $a^{\text{sing}}(u) = K_a(1-3u)^{-n_a}$  with  $K_a \simeq \frac{1}{4}$  and  $n_a = \frac{1}{2}$ . One would then expect a large- $N$  behavior  $a_N \simeq C_a N^{-1/2} 3^N$  with  $C_a \simeq 1/(4\Gamma(\frac{1}{2})) \simeq 0.14$ . We studied the evolution with  $N$  of the PN coefficients  $a_N$  of  $a(u)$  by using the available high-PN results of Refs. [14, 25]. We confirmed the basic exponential growth  $a_N \sim 3^N$ . Indeed, Table VI in Appendix B displays, in its first column, the values of the rescaled PN coefficients  $\hat{a}_N \equiv a_N/3^N$  [with all logarithms replaced by  $\ln(\frac{1}{3})$ ; see below for the logarithmic dependence]. These rescaled coefficients are seen to remain (roughly) of order unity (in absolute magnitude), even up to  $N = 23$  for which  $3^{23} = 0.941432 \times 10^{11}$ . More precisely, we have  $0.1 \lesssim \hat{a}_N \lesssim 1$ , when  $N$  varies between 3 and 20, while, for  $N = 21, 22, 23$ , we have  $|\hat{a}_N| \approx 2.254, 1.459, 3.313$ , respectively. [We do not know if the fact that the latter values are slightly larger than 1 signals the beginning of a growth for very large  $N$ 's.] We did not see any sign of the expected mild decay  $\hat{a}_N \simeq C_a N^{-1/2}$ . This might be due to the more complicated singularity structure (beyond the leading-order power-law) found in [12], or to the fact that the  $N^{-1/2}$  behavior sets in only for very large  $N$ 's. [Note also that, after having factored the clear  $3^N$  growth, the rescaled coefficients  $\hat{a}_N$  behave rather erratically, and do not show any sign of converging towards a simple behavior.] If we were only interested in estimating the PN error for values of  $u$  in the strong-field domain, and for values of  $N$  around 10, we could simply use the simple estimate  $a_N \simeq C_a 3^N$  with  $|C_a| \sim 1$ . However, as we are also interested in knowing what happens when  $u \ll 0$ , we should remember that the PN expansion coefficients run logarithmically with  $u$  as  $u \rightarrow 0$ . We therefore kept the full available high PN information [14, 25] to also inves-

tigate the effect of the logarithms. It is technically convenient to work with the rescaled independent variable  $u_3 \equiv 3u$  (with respect to which the singularity is located at  $u_3 = 1$ ), and expand  $a(u) \equiv a_3(u_3)$  in powers of  $u_3$

$$a(u) = \sum_N (\hat{a}_N + \hat{a}'_N \ln(u_3) + \hat{a}''_N (\ln(u_3))^2 + \dots) u_3^N. \quad (14)$$

Here, the  $\hat{a}_N$  are the same (rescaled) coefficients as above (obtained by replacing  $\ln u$  by  $\ln \frac{1}{3}$ ). The higher logarithmic coefficients  $\hat{a}'_N, \hat{a}''_N, \dots$  are displayed in the other columns of Table VI in Appendix B. We see that the first logarithmic (rescaled) coefficients  $\hat{a}'_N$  are either comparable to the  $\hat{a}_N$ , or slightly smaller in absolute value (the signs, as well as the relative signs, of  $\hat{a}_N$  and  $\hat{a}'_N$  fluctuate). The higher logarithmic terms appear only at  $u^8$ , and their coefficients  $\hat{a}''_N, \dots$  are found to be generally smaller. We shall neglect them in the following. Going back to the original PN-expansion coefficients  $a_N(u)$  of  $a(u) = \sum_N a_N(u) u^N$ , we can then write their combined  $N$  and  $u$  dependence as (neglecting higher logarithms)

$$a_N(u) \simeq (\hat{a}_N + \hat{a}'_N \ln(3u)) 3^N; \quad (15)$$

with  $|\hat{a}_N| \sim |\hat{a}'_N| \sim 1$ . Then, in view of (8), we expect a corresponding approximate asymptotic behavior of the PN expansion coefficients of the precession function  $\rho(u)$  of the type

$$\rho_N(u) \simeq (\hat{\rho}_N + \hat{\rho}'_N \ln(3u)) 3^N; \quad (16)$$

with  $|\hat{\rho}_N| \sim |\hat{\rho}'_N| \sim N^2$ .

We tested this expectation on the 9.5PN-accurate expansion of  $\rho(u)$  given above. An  $N^2$  scaling seems to be in reasonable agreement with the currently known PN coefficients, and we found (using a  $(N-1)^2$  scaling and relying on the 8PN and 9PN nonlogarithmic coefficients to fix the overall coefficient) for the coefficients of  $\rho$  (see Table VII in Appendix B)

$$|\hat{\rho}'_N| \lesssim |\hat{\rho}_N| \sim 2.5 (N-1)^2. \quad (17)$$

A similar study of the PN expansion coefficients of the function  $\bar{d}(u)$  (see Table VIII in Appendix B) leads to a growth similar to the case of the function  $\rho(u)$ , with simply a slightly smaller overall coefficient, i.e.

$$\bar{d}_N(u) \simeq (\hat{\bar{d}}_N + \hat{\bar{d}}'_N \ln(3u)) 3^N; \quad (18)$$

with

$$|\hat{\bar{d}}'_N| \lesssim |\hat{\bar{d}}_N| \sim 0.7 (N-1)^2. \quad (19)$$

Finally, the fact that the EOB potential  $q(u)$  is related to the redshift coefficient  $\delta U^{e^0}(u) \sim a(u)$  by four derivatives [7] suggests, in view of the argument above, that

$$q_N \sim N^4 a_N. \quad (20)$$

We tested this expectation on the 9.5PN-accurate expansion of  $q(u)$  given above. An  $N^4$  [or  $(N-1)^4$ ] scaling

<sup>3</sup> This expectation is based on the usual integral Cauchy formula giving the coefficients of the Laurent expansion of an analytic function. By deforming the contour of integration so that it gets near the (closest) singularity one sees that the Cauchy integral can be approximated by an analogous integral involving  $f^{\text{sing}}(u)$ .

seems to be in reasonable agreement with the currently known PN coefficients, and we found (using mainly the last point for numerically estimating the coefficient; see Table IX in Appendix B)

$$q_N(u) \simeq (\hat{q}_N + \hat{q}'_N \ln(3u)) 3^N; \quad (21)$$

with

$$|\hat{q}'_N| \lesssim |\hat{q}_N| \sim 0.26 (N-1)^4. \quad (22)$$

Let us now turn to estimating the Nth PN remainder  $\epsilon_f^N(u) = O_f(u^N)$  in the PN expansion of some potential:  $f(u) = \sum_{n < N} f_n u^n + \epsilon_f^N(u)$ . As mentioned in [21], the remainder will share the singularity structure of  $f(u)$  and will therefore ultimately blow up as  $f^{\text{sing}}(u) = K_f(1-3u)^{-n_f}$  near the lightring. However, if one is interested (as we are here) in estimating the PN remainder at values of  $u$  significantly away from the singular point, we can neglect any additional factor  $\propto (1-3u)^{-n_f}$  and simply estimate the remainder by the expected (unknown) next term in the PN expansion. Using our results above on the growth with  $N$  of the PN expansion coefficients, we can estimate (by extrapolation on the value of  $N$ ) that the theoretical errors on our 9.5PN expansions Eqs. (5), (6) and (9) are, respectively,

$$\Delta \rho^{9.5\text{PN}} \sim \rho_{10}(u), \quad (23)$$

with

$$|\rho_{10}(u)| \lesssim (1 + |\ln(3u)|) [2.5(N-1)^2 (3u)^N]_{N=10} \\ \simeq 203(1 + |\ln(3u)|) (3u)^{10}. \quad (24)$$

Though, as discussed above, and as can be seen in Tables VI–IX in Appendix B, there is some indication that the coefficient of  $\ln(3u)$  is often smaller than that of the nonlogarithmic term, we have conservatively preferred, in estimating an upper bound on the theoretical error, to assume a relative coefficient equal to one for the logarithmic term. If one were to relax this conservative assumption, one could replace in Eq. (24) [as well as in Eqs. (27), (29) below] the factor  $1 + |\ln(3u)|$  by a factor  $1 + c|\ln(3u)|$  with some positive coefficient  $c < 1$  (e.g.  $c \sim \frac{1}{2}$ ). [Note that, as we are only interested in the domain  $u < \frac{1}{3}$ , we could replace  $|\ln(3u)|$  by  $-\ln(3u)$ .]

We have tested the reasonableness of the estimate (24) by inserting in the  $a(u)$ -related contribution,  $\rho_a(u)$ , to  $\rho(u)$  [see Eqs. (7), (8)] the known 10PN-accurate value of  $a(u)$  straightforwardly computed from the results of Ref. [25] for  $\delta U^{e^0}$ . We found (numerically)

$$\rho_a^{10\text{PN}} \approx [112.44232 + 18.94528 \ln(3u) - 4.08314(\ln(3u))^2 \\ + 0.13206(\ln(3u))^3] (3u)^{10}, \quad (25)$$

which confirms the order of magnitude of our estimate of  $\rho_{10}(u)$ .

Similarly, we get as estimate of the PN error on our 9.5PN expansion of  $\bar{d}(u)$

$$\Delta \bar{d}^{9.5\text{PN}} \sim \bar{d}_{10}(u), \quad (26)$$

with

$$|\bar{d}_{10}(u)| \lesssim 57(1 + |\ln(3u)|) (3u)^{10}. \quad (27)$$

Finally, the corresponding estimate for the 9.5PN expansion of  $q(u)$  (which goes up to  $N = 8.5$ ) reads

$$\Delta q^{9.5\text{PN}} \sim q_9(u), \quad (28)$$

with

$$|q_9(u)| \lesssim 1065(1 + |\ln(3u)|) (3u)^9. \quad (29)$$

#### IV. COMPARING 9.5PN-ACCURATE THEORETICAL RESULTS TO SELF-FORCE NUMERICAL DATA

In the present section we shall compare our 9.5PN-accurate theoretical results to corresponding SF numerical data. First, we display in Table II below the numerical values of the 9.5PN-accurate expansions of the functions  $\rho(u_p)$ ,  $\bar{d}(u_p)$  and  $q(u_p)$  for selected values of the semi-latus rectum  $p \equiv 1/u_p$ . These numerical values are given with twelve significant digits. In addition, for the last four entries, we have also given (on a second line) the digits that our estimated PN error suggests as being meaningful (the PN error being indicated as a last digit, within parentheses).

We then use the theoretical estimates, given in the preceding section, of the PN errors on  $\rho^{9.5\text{PN}}$ ,  $\bar{d}^{9.5\text{PN}}$  and  $q^{9.5\text{PN}}$  to gauge the agreement between these 9.5PN-accurate expansions and some of the currently published corresponding numerical SF estimates, namely: [9] for  $\rho(u)$ , and [29] for  $\bar{d}(u)$ , and  $q(u)$ .

Our comparisons are displayed in Tables III, IV and V. Each Table displays successively:  $p \equiv 1/u_p$ , the difference  $f^{\text{num}}(u_p) - f^{9.5\text{PN}}(u_p)$  between the numerical estimate  $f^{\text{num}}(u_p)$  and our analytical one  $f^{9.5\text{PN}}(u_p)$ , the numerical error estimate  $\Delta f^{\text{num}}$ , the analytical one  $\Delta f^{9.5\text{PN}}$ , and finally the ratio  $[f^{\text{num}}(u_p) - f^{9.5\text{PN}}(u_p)] / \sup(\Delta f^{9.5\text{PN}}, \Delta f^{\text{num}})$ . The latter ratios are decorated with a star when the maximum (estimated) error is of numerical origin.

The fact that the un-starred ratios in the last column are, with very few exceptions<sup>5</sup>, smaller than one confirms the correctness of our analytical results. [The fact that they are often  $\lesssim 0.1$  suggests we overestimated the theoretical error.] Note also that the starred ratios (those for which it is the numerical error which dominates) are, with very few exceptions<sup>6</sup>, smaller than one.

TABLE II. Numerical values for  $\rho$ ,  $\bar{d}$  and  $q$  from our 9.5PN expressions.

$p = 1/u_p$	$\rho^{9.5\text{PN}}$	$\bar{d}^{9.5\text{PN}}$	$q^{9.5\text{PN}}$
6.5	0.671764919305	0.486993641405	0.182950449073
7	0.561736650217	0.382787591949	0.198169550839
8	0.406156070112	0.252398213123	0.169101047037
9	0.305647401966	0.177904676295	0.133125987258
10	0.237602128640	0.131733356706	0.105217407767
12	0.154573521964	0.0801707241916	0.0696067840355
14	0.108052490472	0.0536892308992	0.0493762760810
16	0.0795303790344	0.0383704313535	0.0368759609969
18	0.0608514155206	0.0287425071020	0.0286070525638
20	0.0479869269632	0.0223099143151	0.0228464642737
50	$0.649373236809 \times 10^{-2}$	$0.282840892030 \times 10^{-2}$	$0.339474535246 \times 10^{-2}$
	0.0064937324(5)	0.0028284089(1)	0.00339475(4)
75	$0.275991903932 \times 10^{-2}$	$0.119177507244 \times 10^{-2}$	$0.148216610087 \times 10^{-2}$
	0.002759919039(9)	0.001191775072(3)	0.001482166(1)
100	$0.151587749099 \times 10^{-2}$	$0.652456222249 \times 10^{-3}$	$0.825891422094 \times 10^{-3}$
	0.0015158774910(5)	0.000652456222(2)	0.00082589142(9)
1000	$0.141215418609 \times 10^{-4}$	$0.605194989392 \times 10^{-5}$	$0.802826796636 \times 10^{-5}$
	0.00001412154186085476269(8)	0.00000605194989391653304(2)	0.0000080282679663565(1)

TABLE III. Difference between our 9.5PN results on  $\bar{d}(u_p)$  and a sample of numerical values from Ref. [29].

$p = 1/u_p$	$\bar{d}^{\text{num}} - \bar{d}^{9.5\text{PN}}$	$\Delta \bar{d}^{\text{num}}$	$\Delta \bar{d}^{9.5\text{PN}}$	$(\bar{d}^{\text{num}} - \bar{d}^{9.5\text{PN}})/\text{sup}(\Delta \bar{d})$
6.25	$0.1958 \times 10^{-1}$	$0.38 \times 10^{-5}$	$0.64 \times 10^{-1}$	0.31
7.5	$0.2837 \times 10^{-2}$	$4.5 \times 10^{-8}$	$0.11 \times 10^{-1}$	0.25
9.375	$0.2638 \times 10^{-3}$	$1.4 \times 10^{-9}$	$0.14 \times 10^{-2}$	0.19
12	$0.1814 \times 10^{-4}$	$2.0 \times 10^{-10}$	$0.13 \times 10^{-3}$	0.14
15	$0.1477 \times 10^{-5}$	$1.2 \times 10^{-10}$	$0.15 \times 10^{-4}$	0.097
20	$0.4312 \times 10^{-7}$	$7.1 \times 10^{-11}$	$9.5 \times 10^{-7}$	0.045
25	$0.7734 \times 10^{-9}$	$4.8 \times 10^{-11}$	$1.1 \times 10^{-7}$	0.0070
30	$-0.4376 \times 10^{-9}$	$3.5 \times 10^{-11}$	$1.9 \times 10^{-8}$	-0.023
40	$-0.8033 \times 10^{-10}$	$2.1 \times 10^{-11}$	$1.2 \times 10^{-9}$	-0.070
50	$-0.1030 \times 10^{-10}$	$1.5 \times 10^{-11}$	$1.3 \times 10^{-10}$	-0.078
60	$-0.5004 \times 10^{-11}$	$1.1 \times 10^{-11}$	$2.2 \times 10^{-11}$	-0.22
75	$-0.4399 \times 10^{-12}$	$7.2 \times 10^{-12}$	$2.5 \times 10^{-12}$	-0.061*
100	$-0.2494 \times 10^{-12}$	$4.4 \times 10^{-12}$	$1.5 \times 10^{-13}$	-0.057*
200	$-0.3060 \times 10^{-12}$	$1.3 \times 10^{-12}$	$1.7 \times 10^{-16}$	-0.24*
400	$0.2815 \times 10^{-13}$	$4.0 \times 10^{-13}$	$1.9 \times 10^{-19}$	0.070*

To complete these numerical comparisons by a visual study of the convergence of the PN approximants, we

display in Fig. 1 several successive PN-approximants to the two EOB potentials  $\bar{d}$  and  $q$ , as well as a sample of numerical data points from [29]. There is a visible difference between the behavior of the sequence of PN

<sup>4</sup> While writing up this paper we were informed by Maarten van de Meent that he is finalizing much more accurate numerical computations of  $\rho(u)$  [38].

<sup>5</sup> The only exceptions are:  $p = 75$  for  $q$  and  $p = 25$  for  $\rho$ . For these values the numerical and analytical errors are comparable. Maybe one of the errors is underestimated.

<sup>6</sup> The only exceptions are:  $p = 100$  for  $q$  and  $p = 30$  for  $\rho$ . Maybe one of the errors has been underestimated.

TABLE IV. Difference between our 9.5PN results on  $q(u_p)$  and a sample of numerical values from Ref. [29].

$p = 1/u_p$	$q^{\text{num}} - q^{9.5\text{PN}}$	$\Delta q^{\text{num}}$	$\Delta q^{9.5\text{PN}}$	$(q^{\text{num}} - q^{9.5\text{PN}})/\text{sup}(\Delta q)$
6.25	0.2163	$0.86 \times 10^{-2}$	2.50	0.087
7.5	$0.2821 \times 10^{-1}$	$0.40 \times 10^{-3}$	0.53	0.053
9.375	$0.1227 \times 10^{-2}$	$0.10 \times 10^{-4}$	$0.80 \times 10^{-1}$	0.015
12	$-0.2334 \times 10^{-3}$	$3.8 \times 10^{-7}$	$0.97 \times 10^{-2}$	-0.024
15	$-0.8336 \times 10^{-4}$	$3.0 \times 10^{-8}$	$0.14 \times 10^{-2}$	-0.059
20	$-0.1192 \times 10^{-4}$	$3.4 \times 10^{-8}$	$0.12 \times 10^{-3}$	-0.10
25	$-0.2323 \times 10^{-5}$	$1.5 \times 10^{-8}$	$0.17 \times 10^{-4}$	-0.14
30	$-0.6039 \times 10^{-6}$	$8.2 \times 10^{-9}$	$0.35 \times 10^{-5}$	-0.17
40	$-0.5814 \times 10^{-7}$	$8.1 \times 10^{-10}$	$2.87 \times 10^{-7}$	-0.20
50	$0.2448 \times 10^{-8}$	$8.3 \times 10^{-10}$	$4.1 \times 10^{-8}$	0.060
60	$0.8505 \times 10^{-8}$	$6.0 \times 10^{-10}$	$8.3 \times 10^{-9}$	1.0
75	$0.6899 \times 10^{-8}$	$5.2 \times 10^{-10}$	$1.2 \times 10^{-9}$	5.9
100	$-0.4222 \times 10^{-8}$	$4.2 \times 10^{-10}$	$9.4 \times 10^{-11}$	-10.05*
200	$-0.4066 \times 10^{-10}$	$2.6 \times 10^{-10}$	$2.1 \times 10^{-13}$	-0.16*
400	$-0.4072 \times 10^{-10}$	$1.8 \times 10^{-10}$	$4.7 \times 10^{-16}$	-0.23*

TABLE V. Difference between our 9.5PN results on  $\rho(u_p)$  and the numerical values given in Ref. [9].

$p = 1/u_p$	$\rho^{\text{num}} - \rho^{9.5\text{PN}}$	$\Delta \rho^{\text{num}}$	$\Delta \rho^{9.5\text{PN}}$	$(\rho^{\text{num}} - \rho^{9.5\text{PN}})/\text{sup}(\Delta \rho)$
80	$0.1604 \times 10^{-6}$	$9 \times 10^{-7}$	$4.8 \times 10^{-12}$	0.18*
57.142	$-0.4533 \times 10^{-7}$	$6 \times 10^{-7}$	$1.3 \times 10^{-10}$	-0.076*
50	$0.2676 \times 10^{-6}$	$2 \times 10^{-6}$	$4.7 \times 10^{-10}$	0.13*
44.444	$0.6668 \times 10^{-6}$	$2 \times 10^{-6}$	$1.5 \times 10^{-9}$	0.33*
40	$0.6832 \times 10^{-6}$	$10^{-6}$	$4.1 \times 10^{-9}$	0.68*
36.363	$0.5630 \times 10^{-6}$	$8 \times 10^{-7}$	$1.0 \times 10^{-8}$	0.70*
34.2857	$0.1104 \times 10^{-5}$	$8 \times 10^{-7}$	$1.8 \times 10^{-8}$	1.4*
30	$0.1759 \times 10^{-5}$	$4 \times 10^{-7}$	$6.7 \times 10^{-8}$	4.4*
25	$0.2671 \times 10^{-5}$	$3 \times 10^{-7}$	$3.9 \times 10^{-7}$	6.8
20	$0.4673 \times 10^{-5}$	$5 \times 10^{-7}$	$3.4 \times 10^{-6}$	1.4
19	$0.5111 \times 10^{-5}$	$3 \times 10^{-6}$	$5.6 \times 10^{-6}$	0.92
18	$0.5584 \times 10^{-5}$	$2 \times 10^{-6}$	$9.4 \times 10^{-6}$	0.60
17	$0.6312 \times 10^{-5}$	$4 \times 10^{-6}$	$1.6 \times 10^{-5}$	0.39
16	$0.6621 \times 10^{-5}$	$2 \times 10^{-6}$	$2.9 \times 10^{-5}$	0.23
15	$0.8437 \times 10^{-5}$	$3 \times 10^{-6}$	$5.4 \times 10^{-5}$	0.16
14	$0.8510 \times 10^{-5}$	$2 \times 10^{-6}$	$1.1 \times 10^{-4}$	0.081
13	$0.7202 \times 10^{-5}$	$3 \times 10^{-6}$	$2.1 \times 10^{-4}$	0.034
12	$0.4478 \times 10^{-5}$	$3 \times 10^{-6}$	$4.6 \times 10^{-3}$	0.0097
11	$0.6084 \times 10^{-6}$	$3 \times 10^{-6}$	$1.1 \times 10^{-3}$	0.00057
10	$0.7871 \times 10^{-5}$	$4 \times 10^{-6}$	$2.6 \times 10^{-3}$	0.0030
9	$0.1026 \times 10^{-3}$	$5 \times 10^{-6}$	$7.2 \times 10^{-3}$	0.014
8.5	$0.2515 \times 10^{-3}$	$6 \times 10^{-6}$	$1.2 \times 10^{-2}$	0.020
8	$0.6109 \times 10^{-3}$	$6 \times 10^{-6}$	$2.2 \times 10^{-2}$	0.028
7.5	$0.1456 \times 10^{-2}$	$10^{-5}$	$4.1 \times 10^{-2}$	0.036
7.4	$0.1719 \times 10^{-2}$	$7 \times 10^{-6}$	$4.6 \times 10^{-2}$	0.037
7	$0.3543 \times 10^{-2}$	$10^{-5}$	$7.8 \times 10^{-2}$	0.045
6.8	$0.5096 \times 10^{-2}$	$9 \times 10^{-6}$	$1.0 \times 10^{-1}$	0.049
6.5	$0.8825 \times 10^{-2}$	$10^{-5}$	$1.6 \times 10^{-1}$	0.056
6	$0.2284 \times 10^{-1}$	$4 \times 10^{-5}$	$3.4 \times 10^{-1}$	0.068

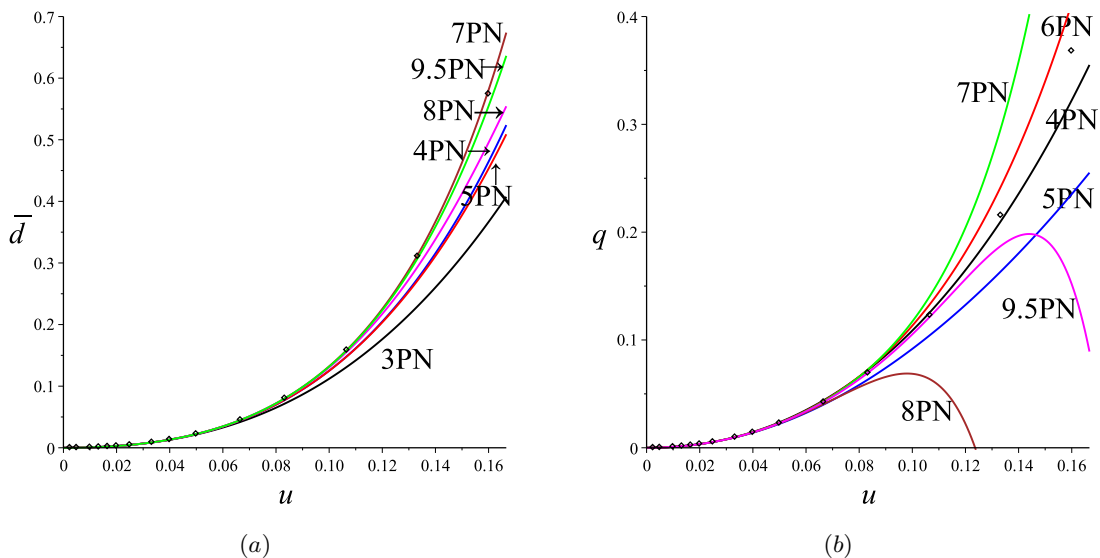


FIG. 1. The behavior of various PN-approximants to the EOB functions  $\bar{d}$  and  $q$  is shown in panels (a) and (b), respectively, and compared to a sample of numerical data points from [29].

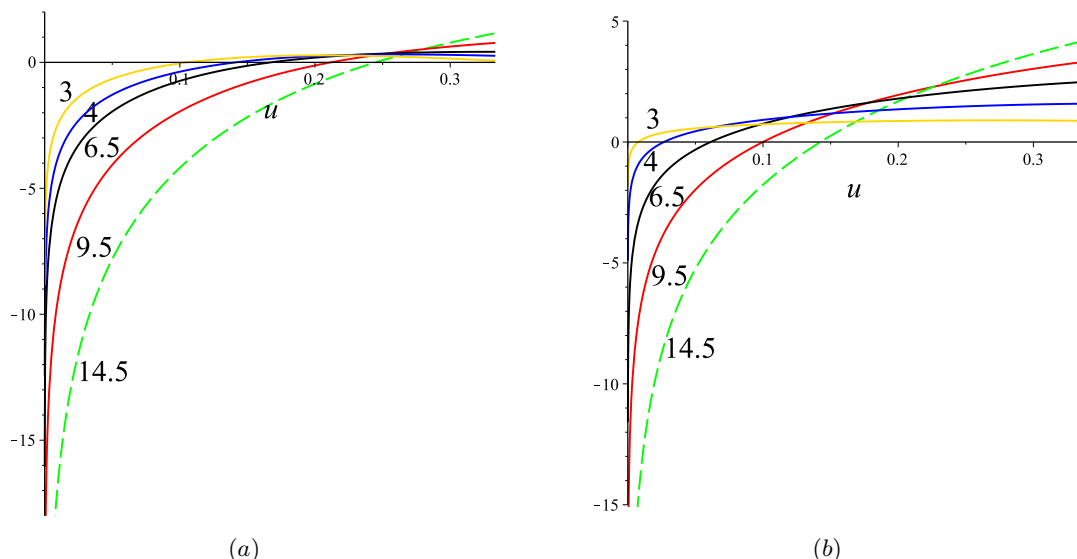


FIG. 2. The (base-10) logarithms of twice the fractional theoretical PN errors on  $\bar{d}$  (panel a), and  $q$  (panel b), for  $N = [3, 4, 6.5, 9.5, 14.5]$  (see text for details).

approximants to  $\bar{d}$  and to  $q$ : while the successive PN approximants to  $\bar{d}$  seem to exhibit the usual erratic, non-monotonic “convergence” toward the exact (numerical) result, the successive PN approximants to  $q$  seem to lose any “convergence” beyond  $u \sim 0.12$ . [Note, however, that some PN approximants are accidentally closer to the numerical results than the other ones: especially, the 7PN approximant for  $\bar{d}$  and the 4PN one for  $q$ .]

The origin of the latter behavior is rooted in the presence of the relatively large additional power-law correc-

tion  $\propto N^4$  in the rescaled PN coefficients  $\hat{q}_N \equiv q_N/3^N$ , see Eq. (21). To better study the influence of these power-law corrections to the basic exponential growth  $\propto 3^N$ , we plot in Figs. 2 (a) and (b), respectively, the fractional PN errors  $\Delta \bar{d}^{NP\text{N}}/\bar{d}$ ,  $\Delta q^{NP\text{N}}/q$ <sup>7</sup>, associated

<sup>7</sup> We use as denominators here the accidentally best PN approximants, i.e.  $\bar{d}^{7\text{PN}}$  and  $q^{4\text{PN}}$ .

with the PN remainders at order  $N$  PN, for the PN orders  $N = 3, 4, 6.5, 9.5$  and  $14.5$ . Here, the cases  $N = 3, 4$  illustrate the currently fully known PN knowledge, the case  $N = 6.5$  illustrates the level of SF PN knowledge [27] for  $\bar{d}$  before the present work,  $N = 9.5$  illustrates the new knowledge brought by the present work, while, finally,  $N = 14.5$  is included (dashed curve) to illustrate what improvement might bring a much more accurate analytical SF computation of  $\bar{d}$  and  $q$ . For clarity, the vertical axis of these figures plot the base-10 logarithm of *twice* the ratios  $\Delta\bar{d}^{NPN}/\bar{d}$ ,  $\Delta q^{NPN}/q$ , so that the crossing of the horizontal axis represents the location on the  $u$  axis where the expected PN error represents about a 50% correction to the exact answer ( $\Delta f/f = \frac{1}{2}$ ). We can then consider that, from the practical point of view, the crossing of the horizontal axis defines the right boundary of the domain of validity of the corresponding PN approximant. For instance, we see on Fig. 2 (a) that our current 9.5PN approximant to  $\bar{d}$  loses its validity beyond  $u \simeq 0.20$ , while Fig. 2 (b) shows that our current 9.5PN approximant to  $q$  loses its validity beyond the significantly smaller value  $u \simeq 0.10$ . We note also that an even much improved 14.5PN analytical knowledge of  $q$  would only displace the right boundary of the so-defined domain of validity to  $u \approx 0.15$ . This behavior makes it clear that high-order PN approximants lose any practical interest for representing the strong-field behavior of the EOB potential  $q(u)$ . On the other hand, as the 4PN approximant to  $q$  is accidentally better than the other ones, it might serve (together with some extra Padé-like factor) as a basis for writing an accurate global analytical representation of  $q$ . Similarly for  $\bar{d}$  when using the 7PN approximant as a basis. Note, however, that it is urgently needed to go beyond the last stable orbit barrier at  $u = \frac{1}{6}$ . As the current, precession-based or redshift-based methods are essentially limited to the range  $0 < u < \frac{1}{6}$ , it would be interesting, as was emphasized early on [8], to use hyperbolic scattering SF computations to explore the EOB potentials in a larger domain of variation.

## V. ANALYTICAL 4PN RESULTS FOR $\delta U^{e^n}$ UP TO $n = 20$

Ref. [33] has shown how to convert the nonlocal interaction appearing at the 4PN order [39, 40] into a specific action-angle Hamiltonian. Moreover, Ref. [33] showed

also how the latter action-angle Hamiltonian could be formally re-expressed in terms of an usual Hamiltonian involving an infinite series of even powers of the radial momentum  $p_r$  of the type

$$\widehat{Q}(r, p_r) = \sum_{n \geq 2} Q_{2n}(u; \nu) p_r^{2n} \quad (30)$$

with a 4PN value of the  $Q$ -potential<sup>8</sup>, of the type

$$Q_{2n}^{4PN}(u; \nu) = u^{5-n} (\nu q_{2n}^c + \nu^2 (q_4' \delta_n^2 + q_6' \delta_n^3) + \nu^3 (q_4'' \delta_n^2 + q_6'' \delta_n^3)) .$$

In this expression the contributions that are nonlinear in  $\nu$  occur only for  $n = 2$  ( $p_r^4$ ) and  $n = 3$  ( $p_r^6$ ), and are only contributed by the *local* piece of the Hamiltonian. The *nonlocal* piece of the 4PN Hamiltonian only contributes terms linear in  $\nu$ , which correspond to the 1SF order. By contrast to the other (locally generated) terms, we see that the 1SF 4PN dynamics contains an infinite number of contributions  $\sim \sum_n \nu q_{2n}^c u^{5-n} p_r^{2n}$ .

Ref. [33] has computed the explicit values of the 4PN coefficients  $q_4^c, q_4', q_4''$  and  $q_6^c, q_6', q_6''$ , and provided general formulas for computing the higher-order coefficients  $q_{2n}^c$ . Ref. [28] has computed the next two (1SF) terms, i.e.  $q_8^c$  and  $q_{10}^c$ , by another route. Namely, they computed by SF methods the 4PN-level contributions to  $\delta U^{e^8}$  and  $\delta U^{e^{10}}$ , and then used the results of [7] to convert these contributions in terms of the corresponding 1SF, 4PN  $Q$ -potential contributions  $q_8^c$  and  $q_{10}^c$ . We have verified that the  $Q$  results of Ref. [28], namely

$$\begin{aligned} q_8^c &= -\frac{35772}{175} + \frac{21668992}{45} \ln(2) \\ &\quad + \frac{6591861}{350} \ln(3) - \frac{27734375}{126} \ln(5), \\ q_{10}^c &= -\frac{231782}{1575} - \frac{408889317632}{212625} \ln(2) \\ &\quad - \frac{22187736351}{28000} \ln(3) + \frac{7835546875}{7776} \ln(5) \\ &\quad + \frac{96889010407}{324000} \ln(7), \end{aligned} \quad (31)$$

do agree with the results obtained by the general formulas in [33].

Using Eqs. (7.5) and (7.7) in [33] we have computed the coefficients  $q_{2n}^c$  for  $n$  varying between 6 and 10. Our results read

<sup>8</sup> The  $Q$  potential corresponds to a term in the effective EOB Hamiltonian, following the standard EOB notation

$$\begin{aligned}
q_{12}^c &= -\frac{252412}{2475} - \frac{71310546875}{24948} \ln(5) + \frac{163796987511}{38500} \ln(3) - \frac{96889010407}{29700} \ln(7) + \frac{7057329658112}{779625} \ln(2) \\
&\approx 0.0018257727627680511315034555270224294943015, \\
q_{14}^c &= -\frac{10281865679266304}{212837625} \ln(2) - \frac{877810440113163}{112112000} \ln(3) + \frac{11259375010387063}{667180800} \ln(7) - \frac{3079166}{45045} \\
&\quad + \frac{1878421041015625}{326918592} \ln(5) \\
&\approx 0.0003789439085938192497702387294880213660917, \\
q_{16}^c &= \frac{417442117895446016}{1915538625} \ln(2) - \frac{827476034230539}{22422400} \ln(3) - \frac{401306}{9009} - \frac{2793081608858259887}{50038560000} \ln(7) \\
&\quad - \frac{1153146534765625}{980755776} \ln(5) \\
&\approx -0.000094237712462701263218285845763487007072, \\
q_{18}^c &= -\frac{22451335308782004224}{28733079375} \ln(2) + \frac{7400249944258160101211}{363771233280000} \ln(11) - \frac{184181968578981640625}{2134124568576} \ln(5) \\
&\quad - \frac{1409537}{49725} + \frac{993339887626452455369}{7423902720000} \ln(7) + \frac{303173836939989783}{896896000} \ln(3) \\
&\approx -0.000012390367224863884457529152672385306211, \\
q_{20}^c &= -\frac{12248956}{692835} - \frac{939831742920786332853797}{3455826716160000} \ln(11) - \frac{967033461070767993388297}{3878989171200000} \ln(7) \\
&\quad + \frac{47970130001158879756288}{19887395653125} \ln(2) - \frac{4894596811860934937067}{3621217600000} \ln(3) + \frac{107731911758417652734375}{182467650613248} \ln(5) \\
&\approx 0.00000218442987916976096395571442115985913. \tag{32}
\end{aligned}$$

Finally, following the procedure outlined in Ref. [7], it is straightforward to determine from the so-determined 4PN-accurate EOB  $Q$ -potential the corresponding 4PN-accurate expression of the redshift coefficient functions  $\delta U^{e^n}(u_p)$ . We found for  $n = 6, 8, 10$  (already given in [28]) and  $n = 12, 14, 16, 18, 20$  (new results):

$$\begin{aligned}
\delta U^{e^6} &= -\frac{5}{2}u_p^3 + \left(-\frac{475}{12} + \frac{41}{128}\pi^2\right)u_p^4 + \left(-\frac{52877}{180} + \frac{178288}{5}\ln(2) - \frac{1994301}{160}\ln(3) - \frac{1953125}{288}\ln(5) - 16\gamma\right. \\
&\quad \left.+ \frac{3385}{4096}\pi^2 - 8\ln(u_p)\right)u_p^5, \\
\delta U^{e^8} &= \frac{15}{64}u_p^3 + \left(-\frac{1171}{384} + \frac{287}{4096}\pi^2\right)u_p^4 + \left(-\frac{55}{12}\ln u_p - \frac{24619}{384} - \frac{55}{6}\gamma + \frac{327115}{196608}\pi^2 - \frac{15967961}{90}\ln(2)\right. \\
&\quad \left.+ \frac{11332791}{1280}\ln(3) + \frac{162109375}{2304}\ln(5)\right)u_p^5, \\
\delta U^{e^{10}} &= \frac{3}{64}u_p^3 + \left(-\frac{115}{128} + \frac{123}{4096}\pi^2\right)u_p^4 + \left(-\frac{329}{240}\ln u_p - \frac{1933}{3840} - \frac{329}{120}\gamma + \frac{172697}{393216}\pi^2 + \frac{18046622551}{27000}\ln(2)\right. \\
&\quad \left.+ \frac{203860829079}{1024000}\ln(3) - \frac{74048828125}{221184}\ln(5) - \frac{678223072849}{9216000}\ln(7)\right)u_p^5, \tag{33}
\end{aligned}$$

and



$$\begin{aligned}
\delta U^{e^{12}} &= \frac{5}{512}u_p^3 + \left(-\frac{1909}{3072} + \frac{533}{32768}\pi^2\right)u_p^4 \\
&+ \left(-\frac{104557}{46080} + \frac{1655}{8192}\pi^2 - \frac{95932245107}{36000}\ln(2) - \frac{211}{320}\ln(u_p) - \frac{4936871473659}{4096000}\ln(3) + \frac{678223072849}{819200}\ln(7)\right. \\
&\left. - \frac{211}{160}\gamma + \frac{285888671875}{294912}\ln(5)\right)u_p^5, \\
\delta U^{e^{14}} &= \left(-\frac{5}{12} + \frac{41}{4096}\pi^2\right)u_p^4 \\
&+ \left(-\frac{135071}{107520} + \frac{4311583788974229}{1605632000}\ln(3) - \frac{2758333237276883}{637009920}\ln(7) + \frac{195921190766921}{15876000}\ln(2)\right. \\
&\left. - \frac{2984729833984375}{1560674304}\ln(5) + \frac{89395}{786432}\pi^2 - \frac{73}{192}\ln(u_p) - \frac{73}{96}\gamma\right)u_p^5, \\
\delta U^{e^{16}} &= -\frac{45}{16384}u_p^3 + \left(\frac{7011}{1048576}\pi^2 - \frac{9525}{32768}\right)u_p^4 \\
&+ \left(\frac{3606265}{50331648}\pi^2 - \frac{187}{384}\gamma - \frac{866799}{1146880} + \frac{151266508326642969}{25690112000}\ln(3) + \frac{30647775337890625}{24970788864}\ln(5)\right. \\
&\left. - \frac{187}{768}\ln(u_p) + \frac{132130740829369331}{9437184000}\ln(7) - \frac{9809130397488463}{190512000}\ln(2)\right)u_p^5, \\
\delta U^{e^{18}} &= -\frac{55}{16384}u_p^3 + \left(-\frac{20755}{98304} + \frac{4961}{1048576}\pi^2\right)u_p^4 \\
&+ \left(-\frac{1985885}{4128768} + \frac{1632805}{33554432}\pi^2 - \frac{685}{4096}\ln(u_p) - \frac{81402749386839761113321}{21574761578496000}\ln(11) - \frac{685}{2048}\gamma\right. \\
&+ \frac{926296539361158203125}{57532697542656}\ln(5) - \frac{13828959005709035994883}{440301256704000}\ln(7) \\
&\left. - \frac{27896787814453074891}{411041792000}\ln(3) + \frac{14107331956051038263}{82301184000}\ln(2)\right)u_p^5, \\
\delta U^{e^{20}} &= -\frac{429}{131072}u_p^3 + \left(-\frac{124795}{786432} + \frac{29315}{8388608}\pi^2\right)u_p^4 \\
&+ \left(-\frac{395456141}{1238630400} - \frac{240907615282410313097}{503884800000}\ln(2) - \frac{29689}{245760}\ln(u_p) - \frac{230415740222184068359375}{2071177111535616}\ln(5)\right. \\
&+ \frac{1551270323409360145587}{5872025600000}\ln(3) + \frac{2290704611907930887405849}{44030125670400000}\ln(7) + \frac{21408923088738857172803423}{431495231569920000}\ln(11) \\
&\left. + \frac{7017461}{201326592}\pi^2 - \frac{29689}{122880}\gamma\right)u_p^5. \tag{34}
\end{aligned}$$

The conversion of these results in terms of the  $e^n$  expansion of  $\delta z_1 = -\delta U/U_0^2$  reads

$$\begin{aligned}
\delta z_1^{e^{12}} &= \frac{25}{512} u_p^3 + \left( -\frac{533}{32768} \pi^2 + \frac{3391}{3072} \right) u_p^4 \\
&+ \left( -\frac{7973}{32768} \pi^2 + \frac{95932245107}{36000} \ln(2) + \frac{211}{320} \ln(u_p) + \frac{204491}{23040} + \frac{4936871473659}{4096000} \ln(3) - \frac{678223072849}{819200} \ln(7) \right. \\
&\left. + \frac{211}{160} \gamma - \frac{285888671875}{294912} \ln(5) \right) u_p^5, \\
\delta z_1^{e^{14}} &= \frac{15}{512} u_p^3 + \left( \frac{485}{768} - \frac{41}{4096} \pi^2 \right) u_p^4 \\
&+ \left( -\frac{4311583788974229}{1605632000} \ln(3) + \frac{2758333237276883}{637009920} \ln(7) + \frac{104249}{26880} - \frac{195921190766921}{15876000} \ln(2) \right. \\
&\left. + \frac{2984729833984375}{1560674304} \ln(5) - \frac{104155}{786432} \pi^2 + \frac{73}{192} \ln(u_p) + \frac{73}{96} \gamma \right) u_p^5, \\
\delta z_1^{e^{16}} &= \frac{315}{16384} u_p^3 + \left( -\frac{7011}{1048576} \pi^2 + \frac{13215}{32768} \right) u_p^4 \\
&+ \left( -\frac{4108105}{50331648} \pi^2 + \frac{187}{384} \gamma + \frac{586431}{286720} - \frac{151266508326642969}{25690112000} \ln(3) - \frac{30647775337890625}{24970788864} \ln(5) + \frac{187}{768} \ln(u_p) \right. \\
&\left. - \frac{132130740829369331}{9437184000} \ln(7) + \frac{9809130397488463}{190512000} \ln(2) \right) u_p^5, \\
\delta z_1^{e^{18}} &= \frac{55}{4096} u_p^3 + \left( -\frac{4961}{1048576} \pi^2 + \frac{27205}{98304} \right) u_p^4 \\
&+ \left( \frac{685}{4096} \ln(u_p) - \frac{1829605}{33554432} \pi^2 + \frac{81402749386839761113321}{21574761578496000} \ln(11) + \frac{4960745}{4128768} + \frac{685}{2048} \gamma \right. \\
&\left. - \frac{926296539361158203125}{57532697542656} \ln(5) + \frac{13828959005709035994883}{440301256704000} \ln(7) + \frac{27896787814453074891}{411041792000} \ln(3) \right. \\
&\left. - \frac{14107331956051038263}{82301184000} \ln(2) \right) u_p^5, \\
\delta z_1^{e^{20}} &= \frac{1287}{131072} u_p^3 + \left( \frac{157201}{786432} - \frac{29315}{8388608} \pi^2 \right) u_p^4 \\
&+ \left( \frac{234834179}{309657600} + \frac{240907615282410313097}{503884800000} \ln(2) + \frac{29689}{245760} \ln(u_p) + \frac{230415740222184068359375}{2071177111535616} \ln(5) \right. \\
&\left. - \frac{1551270323409360145587}{5872025600000} \ln(3) - \frac{2290704611907930887405849}{44030125670400000} \ln(7) - \frac{21408923088738857172803423}{431495231569920000} \ln(11) \right. \\
&\left. - \frac{7764317}{201326592} \pi^2 + \frac{29689}{122880} \gamma \right) u_p^5. \tag{35}
\end{aligned}$$

## VI. DISCUSSION

We have improved the analytical knowledge of the eccentricity-expansion of the Detweiler-Barack-Sago redshift invariant (in a Schwarzschild spacetime) in several different ways. First, we have analytically computed the  $e^2$  and  $e^4$  contributions to the 1SF contribution to the average redshift up to the 9.5th post-Newtonian order (included). For the  $e^2$  contribution this is an improvement by three PN orders compared to previous knowledge. For the  $e^4$  contribution this is an improvement by five-and-a-half PN orders compared to previous knowledge. We have also provided for the first time the  $e^{12}$ ,  $e^{14}$ ,  $e^{16}$ ,  $e^{18}$ , and  $e^{20}$  contributions to the 4PN approximation. We have then converted this new analytical information in

---

terms of corresponding dynamically relevant effective-one-body (EOB) potentials:  $\bar{d}(u)$ ,  $\rho(u)$  and  $q(u)$ .

We have shown how to estimate the order of magnitude of the coefficients of the PN expansions of the EOB potentials  $a(u)$ ,  $\rho(u)$ ,  $\bar{d}(u)$ , and  $q(u)$ . See Eqs. (15), (16), (17), (18), (19), (21), (22). We then used this knowledge to estimate the remainder terms in our current 9.5PN-accurate expansions. Let us note that it would be interesting to refine our estimates, and, in particular, to numerically study the behavior of the rescaled coefficients  $\hat{a}_N \equiv a_N/3^N$  for very large values of  $N$ . We gave arguments suggesting a slow decrease  $\hat{a}_N \sim N^{-\frac{1}{2}}$ , but found no evidence for it up to  $N = 23$ . This might be due to a transient behavior proportional to  $(1 - 3u)^{-1} = \sum_N (3u)^N$  of  $a(u)$  before it

zooms on its near-lightning behavior  $\propto (1 - 3u)^{-\frac{1}{2}}$ . [Indeed, Ref. [12] found that the rescaled function  $\hat{a}_E(u)$  increases rather steeply (from 1 to  $\simeq 10$ ) as  $u$  varies between 0 and  $\frac{1}{3}$ . This increase is roughly proportional (modulo an essentially linear function) to  $\propto (1 - 3u)^{-\frac{1}{2}}$  (before levelling off) and might explain the transient appearance of a growth of  $a(u)$  roughly proportional to  $(1 - 3u)^{-\frac{1}{2}} E(u) = (1 - 2u)(1 - 3u)^{-1}$ .]

We compared our 9.5PN-accurate analytical representations of the functions  $\rho(u)$ ,  $\bar{d}(u)$ , and  $q(u)$  to the currently published numerical SF evaluations of these functions [9, 29]. The results of our comparisons are given in Tables III, IV and V. The analytical/numerical agreement is fully satisfactory, in view of the estimated theoretical and numerical errors. [It suggests that both types of errors have been often slightly overestimated.]

We studied the convergence of the successive PN approximants to both  $\bar{d}(u)$  and  $q(u)$ , see the two panels of Fig. 1. The newest result of this study is the particularly unsatisfactory convergence, near  $u \sim 0.1$ , of the successive PN approximants to  $q(u)$ . We explained this worst-than-usual behavior of PN approximants by the presence of a large power-law subleading correction  $\propto N^4$  to the exponential growth  $\propto 3^N$  of the PN coefficients of  $q(u)$ . This  $N^4$  factor underlies the poor accuracy of the 9.5PN approximant in the relatively weak-field domain  $u \sim 0.1$ . See second panel of Fig. 2. We leave to future work the construction of accurate hybrid PN-SF analytical representations of the EOB potentials  $\bar{d}(u)$ , and  $q(u)$ , valid both in the weak-field and the strong-field domains.

We emphasized that a comparison between our 9.5PN analytical computation of the precession function  $\rho(u)$  (which combines SF theory with the eccentric first law [7]) and of high-accuracy SF numerical computations of the purely dynamical precession of eccentric orbits (as in [9]) would be a useful check of the assumptions underlying the theoretical bridges (EOB and the first law of binary mechanics) which have been recently quite useful for connecting SF and PN results.

We recalled that the use of precession-based or redshift-based SF methods currently limit the computation of the EOB potentials  $\bar{d}(u)$  and  $q(u)$  to the medium-strong-field domain  $0 < u < \frac{1}{6}$ . It would be interesting, as was pointed out in [8], to use hyperbolic scattering SF computations to explore the EOB potentials in a larger domain of variation. In particular, one would like to confirm the conjecture [12] that  $\bar{d}(u)$  and  $\rho(u)$  [which are both related to  $a''(u)$ ] diverge (when  $u \rightarrow \frac{1}{3}$ ) like  $(1 - 3u)^{-\frac{5}{2}}$ . One similarly expects that  $q(u)$  [related to  $a''''(u)$ ] will diverge like  $(1 - 3u)^{-\frac{9}{2}}$ . The power-law growths found in the rescaled PN coefficients  $\hat{d}_N, \hat{\rho}_N, \hat{q}_N$  suggest such strong lightning singularities (though there is a mismatch of a missing factor  $N^{-\frac{1}{2}}$  in the observed growths).

## Appendix A: Combined use of RWZ approach, PN solutions and MST technique

Our analytical computation of the conservative SF effects along an eccentric orbit in a Schwarzschild background follows the approach originally introduced in Ref. [18] and then standardized in a sequence of successive works [14, 19, 21–23, 25]. The main steps (together with some of the most important computational details) are listed below [see our previous papers for the notation, which we follow here.]

The Detweiler-Barack-Sago [31, 32] inverse redshift invariant function for eccentric orbits is defined as

$$U \left( m_2 \Omega_r, m_2 \Omega_\phi, \frac{m_1}{m_2} \right) = \frac{\oint dt}{\oint d\tau} = \frac{T_r}{\mathcal{T}_r}, \quad (\text{A1})$$

where all quantities refer to the perturbed spacetime metric (see Eq. (A3) below). The symbol  $\oint$  denotes an integral over a radial period (from periastron to periastron) so that  $T_r = \oint dt$  denotes the coordinate-time period and  $\mathcal{T}_r = \oint d\tau$  the proper-time period. The first-order SF contribution  $\delta U$  to the function (A1), defined by

$$U \left( m_2 \Omega_r, m_2 \Omega_\phi, \frac{m_1}{m_2} \right) = U_0(m_2 \Omega_r, m_2 \Omega_\phi) + \frac{m_1}{m_2} \delta U(m_2 \Omega_r, m_2 \Omega_\phi) + O \left( \frac{m_1^2}{m_2^2} \right), \quad (\text{A2})$$

represents a gauge-invariant measure of the  $O(m_1/m_2)$  conservative SF effect on eccentric orbits. It is a function of the two fundamental frequencies of the orbit, i.e., the radial frequency  $\Omega_r = 2\pi/T_r$  and the mean azimuthal frequency  $\Omega_\phi = \Phi/T_r$ , where  $\Phi$  is the angular advance during one radial period  $T_r$ , and is conveniently expressed in terms of the dimensionless semi-latus rectum  $p$  and the eccentricity  $e$  of the unperturbed orbit, i.e.,  $\delta U = \delta U(p, e)$ . It is given in terms of the  $O(m_1/m_2)$  metric perturbation  $h_{\mu\nu}$ , where

$$g_{\mu\nu}(x^\alpha; m_1, m_2) = g_{\mu\nu}^{(0)}(x^\alpha; m_2) + \frac{m_1}{m_2} h_{\mu\nu}(x^\alpha) + O \left( \frac{m_1^2}{m_2^2} \right), \quad (\text{A3})$$

[with  $g_{\mu\nu}^{(0)}(x^\alpha; m_2)$  being the Schwarzschild metric of mass  $m_2$ ] by the following time average

$$\delta U(p, e) = \frac{1}{2} U_0^2 \langle h_{uk} \rangle_t. \quad (\text{A4})$$

Here, we have expressed  $\delta U$  (which is originally defined as a *proper* time  $\tau$  average [32]) in terms of the *coordinate* time  $t$  average of the mixed contraction  $h_{uk} = h_{\mu\nu} u^\mu k^\nu$  where  $u^\mu \equiv u^t k^\mu$ ,  $u^t = dt/d\tau$  and  $k^\mu \equiv \partial_t + dr/dt \partial_r + d\phi/dt \partial_\phi$ . [Note that in the present eccentric case the so-defined  $k^\mu = u^\mu/u^t$  is no longer a Killing vector.] In Eq.

(A4) we considered  $\delta U$  as a function of the dimensionless semi-latus rectum  $p$  and eccentricity  $e$  (in lieu of  $m_2\Omega_r$ ,  $m_2\Omega_\phi$ ) of the *unperturbed* orbit, as is allowed in a first-order SF quantity. In addition,  $U_0$  denotes the proper-time average of  $u^t = dt/d\tau$  along the unperturbed orbit, i.e., the ratio  $U_0 = T_r/\mathcal{T}_r|_{\text{unperturbed}}$ .

to the (coordinate-time) averaged redshift  $z_1$

$$z_1 = \left\langle \frac{d\tau}{dt} \right\rangle_t = \left( \left\langle \frac{dt}{d\tau} \right\rangle_\tau \right)^{-1} = U^{-1}, \quad (\text{A5})$$

namely

$$\delta z_1 = -\frac{\delta U}{U_0^2} = -\frac{1}{2}\langle h_{uk} \rangle_t. \quad (\text{A6})$$

### 1. Unperturbed particle motion

Up to order  $e^4$  included, the unperturbed *eccentric* particle motion  $r_0(t)$ ,  $\phi_0(t)$  is explicitly given by

The correction  $\delta U$  is equivalent to the correction  $\delta z_1$

$$\begin{aligned} r_0(t) &= R_0 + eR_1(\cos(\Omega_{r0}t) - 1) + e^2R_2(\cos(2\Omega_{r0}t) - 1) \\ &\quad + e^3[R_{3c3}(\cos(3\Omega_{r0}t) - 1) + R_{3c1}(\cos(\Omega_{r0}t) - 1) + R_{3s1}t \sin(\Omega_{r0}t)] \\ &\quad + e^4[R_{4c2}(\cos(2\Omega_{r0}t) - 1) + R_{4s2}t \sin(2\Omega_{r0}t) + R_{4c4}(\cos(4\Omega_{r0}t) - 1)], \\ \phi_0(t) &= \Omega_{\phi 0}t + e\Phi_1 \sin(\Omega_{r0}t) + e^2\Phi_2 \sin(2\Omega_{r0}t) \\ &\quad + e^3[\Phi_{3c1}t \cos(\Omega_{r0}t) + \Phi_{3s1} \sin(\Omega_{r0}t) + \Phi_{3s3} \sin(3\Omega_{r0}t)] \\ &\quad + e^4[\Phi_{4c2}t \cos(2\Omega_{r0}t) + \Phi_{4s2} \sin(2\Omega_{r0}t) + \Phi_{4s4} \sin(4\Omega_{r0}t)], \end{aligned} \quad (\text{A7})$$

with

$$\begin{aligned} R_0 &= m_2p(1 + e + e^2 + e^3 + e^4), \\ R_1 &= m_2p, \\ R_2 &= -m_2p \frac{p^2 - 11p + 26}{2(p-2)(p-6)}, \\ R_{3c1} &= m_2p \frac{10p^4 - 124p^3 + 385p^2 + 220p - 1404}{16(p-2)^2(p-6)^2}, \\ R_{3c3} &= m_2p \frac{6p^4 - 132p^3 + 1023p^2 - 3292p + 3708}{16(p-2)^2(p-6)^2}, \\ R_{3s1} &= m_2 \frac{3(2p^3 - 32p^2 + 165p - 266)}{4p(p-6)^{3/2}(p-2)}, \\ R_{4c2} &= -m_2p \frac{p^5 - 4p^4 - 203p^3 + 2337p^2 - 9192p + 12228}{6(p-2)^2(p-6)^3}, \\ R_{4c4} &= -m_2p \frac{168630p^2 - 310092p - 46697p^3 + 6951p^4 - 528p^5 + 16p^6 + 226968}{48(p-2)^3(p-6)^3}, \\ R_{4s2} &= -m_2 \frac{3(2p^3 - 32p^2 + 165p - 266)(p^2 - 11p + 26)}{4p(p-6)^{5/2}(p-2)^2}, \end{aligned} \quad (\text{A8})$$

and

$$\begin{aligned}
\Phi_1 &= -2 \frac{(p-3)p^{1/2}}{(p-2)(p-6)^{1/2}}, \\
\Phi_2 &= \frac{1}{4} \frac{(5p^3 - 64p^2 + 250p - 300)p^{1/2}}{(p-6)^{3/2}(p-2)^2}, \\
\Phi_{3c1} &= \frac{3}{2} \frac{(p-3)(2p^3 - 32p^2 + 165p - 266)}{p^{3/2}(p-6)^2(p-2)^2}, \\
\Phi_{3s1} &= \frac{1}{8} \frac{(2p^5 - 74p^4 + 855p^3 - 4261p^2 + 9264p - 6948)p^{1/2}}{(p-6)^{5/2}(p-2)^3}, \\
\Phi_{3s3} &= -\frac{1}{24} \frac{(26p^5 - 594p^4 + 5187p^3 - 21545p^2 + 42480p - 31860)p^{1/2}}{(p-6)^{5/2}(p-2)^3}, \\
\Phi_{4c2} &= -\frac{3}{8} \frac{(5p^3 - 64p^2 + 250p - 300)(2p^3 - 32p^2 + 165p - 266)}{p^{3/2}(p-6)^3(p-2)^3}, \\
\Phi_{4s2} &= -\frac{1}{48} \frac{(22p^7 - 972p^6 + 16191p^5 - 136892p^4 + 644034p^3 - 1695084p^2 + 2313960p - 1262160)p^{1/2}}{(p-6)^{7/2}(p-2)^4}, \\
\Phi_{4s4} &= \frac{1}{192} \frac{(206p^7 - 6804p^6 + 93327p^5 - 687580p^4 + 2932674p^3 - 7231980p^2 + 9545448p - 5206608)p^{1/2}}{(p-6)^{7/2}(p-2)^4}. \quad (\text{A9})
\end{aligned}$$

The  $m_2$ -adimensionalized orbital frequencies of the radial and azimuthal motions are given by

$$\begin{aligned}
\Omega_{r0} &= \frac{(p-6)^{1/2}}{p^2} - \frac{3}{4} \frac{(2p^3 - 32p^2 + 165p - 266)}{p^2(p-2)(p-6)^{3/2}} e^2 \\
&\quad + \frac{3}{64} \frac{(8p^7 - 336p^6 + 5724p^5 - 51456p^4 + 263441p^3 - 764550p^2 + 1152396p - 681224)}{p^2(p-6)^{7/2}(p-2)^3} e^4, \\
\Omega_{\phi 0} &= \frac{1}{p^{3/2}} - \frac{3}{2} \frac{(p^2 - 10p + 22)}{(p-2)(p-6)p^{3/2}} e^2 + \frac{3}{16} \frac{(2p^6 - 72p^5 + 993p^4 - 6786p^3 + 24250p^2 - 42528p + 27864)}{(p-2)^3(p-6)^3p^{3/2}} e^4, \quad (\text{A10})
\end{aligned}$$

respectively. Finally, the (unperturbed) redshift variable  $U_0 = T_{r0}/\mathcal{T}_{r0}$  is given by

$$\begin{aligned}
U_0 &= \frac{p^{1/2}}{(p-3)^{1/2}} - \frac{3}{2} \frac{(p^2 - 10p + 22)p^{1/2}}{(p-2)(p-6)(p-3)^{3/2}} e^2 \\
&\quad - \frac{3}{8} \frac{(p^6 - 6p^5 - 163p^4 + 2188p^3 - 10565p^2 + 22860p - 18612)p^{1/2}}{(p-2)^3(p-6)^3(p-3)^{5/2}} e^4 + O(e^5). \quad (\text{A11})
\end{aligned}$$

## 2. Source terms

We first compute the (nine) source terms in the RWZ perturbation approach, namely

$$A_{lm}^{(0)}(t, r) = m_1 u^t \left( \frac{dr_0}{dt} \right)^2 \frac{1}{(r - 2m_2)^2} \delta(r - r_0(t)) e^{-im\phi_0(t)} Y_{lm}^* \left( \frac{\pi}{2} \right), \quad (\text{A12})$$

etc., where  $Y_{lm}(\theta)$  denotes the value of the usual spherical harmonics at  $\phi = 0$ , while  $Y'_{lm}(\theta)$  denotes its  $\theta$ -derivative, and consider then their Fourier transform

$$A_{lm\omega}^{(0)}(r) = \int_{-\infty}^{\infty} e^{i\omega t} A_{lm}^{(0)}(t, r) dt, \quad (\text{A13})$$

etc. The result (after expanding in powers of the eccentricity through  $e^4$ ) is of the form

$$A_{lm\omega}^{(0)}(r) = \sum_{n=-4}^4 [c_n(r)\delta_n + \tilde{c}_n(r)\delta'_n], \quad c_n(r) = \sum_{k=0}^4 c_{n,k}(r_0)\delta^{(k)}(r - r_0), \quad \tilde{c}_n(r) = \sum_{k=0}^4 d_{n,k}(r_0)\delta^{(k)}(r - r_0), \quad (\text{A14})$$

with  $r_0 = m_2 p$  and

$$\delta_n = \delta(\omega - \omega_{m,n}), \quad \omega_{m,n} = m\Omega_{\phi_0} + n\Omega_{r_0}, \quad (\text{A15})$$

so that  $\delta_{n=0} = \delta(\omega - m\Omega_{\phi_0})$ ,  $\delta_{n=+1} = \delta(\omega - m\Omega_{\phi_0} - \Omega_{r_0})$ , etc. The various quantities  $\delta_n$ ,  $c_n(r)$ , etc. also depend on  $l, m, \omega$ , even if not shown explicitly to ease the notation. With the coefficients  $A_{lm\omega}^{(0)}(r)$ , etc. one computes the odd- and even-Zerilli sources. In order to write a single Regge-Wheeler (RW) equation for both cases, the even-Zerilli sources should be mapped into certain (different) even sources, the associated map requiring an extra  $r$ -derivative.

Summarizing, the odd sources are of the form

$$\begin{aligned} S_{lm\omega}^{(\text{odd})}(r) &= \sum_{n=-4}^4 s_n^{(\text{odd})}(r)\delta_n + \sum_{n=-2}^2 \tilde{s}_n^{(\text{odd})}(r)\delta'_n, \\ s_n^{(\text{odd})}(r) &= \sum_{k=0}^5 s_{n,k}^{(\text{odd})}(r_0)\delta^{(k)}(r-r_0), \quad \tilde{s}_n^{(\text{odd})}(r) = \sum_{k=0}^3 \tilde{s}_{n,k}^{(\text{odd})}(r_0)\delta^{(k)}(r-r_0), \end{aligned} \quad (\text{A16})$$

while the even sources are of the form

$$\begin{aligned} S_{lm\omega}^{(\text{even})}(r) &= \sum_{n=-4}^4 s_n^{(\text{even})}(r)\delta_n + \sum_{n=-2}^2 \tilde{s}_n^{(\text{even})}(r)\delta'_n, \\ s_n^{(\text{even})}(r) &= \sum_{k=0}^6 s_{n,k}^{(\text{even})}(r_0)\delta^{(k)}(r-r_0), \quad \tilde{s}_n^{(\text{even})}(r) = \sum_{k=0}^4 \tilde{s}_{n,k}^{(\text{even})}(r_0)\delta^{(k)}(r-r_0), \end{aligned} \quad (\text{A17})$$

both of them satisfying the RW equation

$$\mathcal{L}_{(\text{RW})}^{(r)}[R_{lm\omega}^{(\text{even/odd})}] = S_{lm\omega}^{(\text{even/odd})}(r), \quad (\text{A18})$$

where  $\mathcal{L}_{(\text{RW})}^{(r)}$  denotes the RW operator

$$\mathcal{L}_{(\text{RW})}^{(r)} = \frac{d^2}{dr_*^2} + [\omega^2 - V_{(\text{RW})}(r)], \quad (\text{A19})$$

with  $d/dr_* = f(r)d/dr$  (with  $f(r) \equiv 1 - 2m_2/r$ ), and a RW potential

$$V_{(\text{RW})}(r) = f(r) \left( \frac{l(l+1)}{r^2} - \frac{6m_2}{r^3} \right). \quad (\text{A20})$$

### 3. Green function

The Green function of the RW equation (A18) reads as

$$G_{lm\omega}(r, r') = \frac{1}{W_{lm\omega}} [R_{\text{in}}^{lm\omega}(r)R_{\text{up}}^{lm\omega}(r')H(r'-r) + R_{\text{in}}^{lm\omega}(r')R_{\text{up}}^{lm\omega}(r)H(r-r')], \quad (\text{A21})$$

satisfying  $\mathcal{L}_{\text{RW}}^{(r)}G_{lm\omega}(r, r') = f(r)\delta(r-r')$ , in terms of two, specially chosen, independent homogeneous solutions  $R_{\text{in}}^{lm\omega}(r)$  and  $R_{\text{up}}^{lm\omega}(r)$  of the RW operator (A19). Here

$$W_{lm\omega} = f(r) [R_{\text{in}}^{lm\omega}(r)R_{\text{up}}^{lm\omega}(r) - R_{\text{in}}^{lm\omega}(r)R_{\text{up}}^{lm\omega}(r)] \quad (\text{A22})$$

is the (constant) Wronskian and  $H(x)$  denotes the Heaviside step function. Both even-parity and odd-parity solutions

$$R_{lm\omega}^{(\text{even/odd})}(r) = \int dr' \frac{G_{lm\omega}(r, r')}{f(r')} S_{lm\omega}^{(\text{even/odd})}(r') \quad (\text{A23})$$

are then uniquely determined by selecting  $R_{\text{in}}^{lm\omega}(r)$  as the homogeneous solution which is incoming from infinity, i.e., purely ingoing on the horizon, and  $R_{\text{up}}^{lm\omega}(r)$  as that one which is upgoing from the horizon, i.e., purely outgoing at

infinity. The even source terms come with a factor  $Y_{lm}^*$ , while the odd ones with a factor  $Y_{lm}^{\prime*}$ , which can then be factored out. Recalling that

$$\int h(x)\delta^{(k)}(x-x_0)dx = (-1)^k \lim_{x \rightarrow x_0} \left( \frac{d^k h(x)}{dx^k} \right), \quad (\text{A24})$$

we find, for example (the subscript  $-$  denoting a left limit  $r \rightarrow r_0^-$ )

$$R_{lm\omega,-}^{(\text{even/odd})}(r) = \sum_{n,k} [s_{n,k}^{(\text{even/odd})}(r_0)\delta_n + \tilde{s}_{n,k}^{(\text{even/odd})}(r_0)\delta'_n] \frac{R_{\text{in}}^{lm\omega}(r)}{W_{lm\omega}} (-1)^k \lim_{r' \rightarrow r_0} \left( \frac{d^k R_{\text{up}}^{lm\omega}(r')}{f(r')} \right). \quad (\text{A25})$$

Next, replacing the second (and higher) radial derivatives of  $R_{\text{in/up}}^{lm\omega}(r)$  by using the RW equation leads to expressions of the type

$$\begin{aligned} R_{lm\omega,-}^{(\text{even})}(r) &= \sum_n \frac{Y_{lm}^* \left( \frac{\pi}{2} \right)}{W_{lm\omega}} \left[ J_{\text{up}(\text{even})}^{lm\omega,n}(r_0)\delta_n + \tilde{J}_{\text{up}(\text{even})}^{lm\omega,n}(r_0)\delta'_n \right] R_{\text{in}}^{lm\omega}(r), \\ R_{lm\omega,-}^{(\text{odd})}(r) &= \sum_n \frac{Y_{lm}^{\prime*} \left( \frac{\pi}{2} \right)}{W_{lm\omega}} \left[ J_{\text{up}(\text{odd})}^{lm\omega,n}(r_0)\delta_n + \tilde{J}_{\text{up}(\text{odd})}^{lm\omega,n}(r_0)\delta'_n \right] R_{\text{in}}^{lm\omega}(r), \end{aligned} \quad (\text{A26})$$

where

$$\begin{aligned} J_{\text{up}(\text{even/odd})}^{lm\omega,n}(r_0) &= J_{R_{\text{up}(\text{even/odd})}}^{lm\omega,n}(r_0)R_{\text{up}}^{lm\omega}(r_0) + J_{R'_{\text{up}(\text{even/odd})}}^{lm\omega,n}(r_0)R'_{\text{up}}^{lm\omega}(r_0), \\ \tilde{J}_{\text{up}(\text{even/odd})}^{lm\omega,n}(r_0) &= \tilde{J}_{R_{\text{up}(\text{even/odd})}}^{lm\omega,n}(r_0)R_{\text{up}}^{lm\omega}(r_0) + \tilde{J}_{R'_{\text{up}(\text{even/odd})}}^{lm\omega,n}(r_0)R'_{\text{up}}^{lm\omega}(r_0), \end{aligned} \quad (\text{A27})$$

and similarly for  $R_{lm\omega,+}^{(\text{even/odd})}(r)$ .

#### 4. Computing $h_{uk}$

Next, one can compute the components of the perturbed metric and, in particular, the contraction  $h_{uk}$  needed to construct the Detweiler's redshift invariant. One has at a generic spacetime point

$$\begin{aligned} h_{uk}(t, r, \theta, \phi) &= \sum_{lm} [h_{uk}^{lm(\text{even})}(t, r, \theta, \phi) + h_{uk}^{lm(\text{odd})}(t, r, \theta, \phi)], \\ h_{uk}^{lm(\text{even})}(t, r, \theta, \phi) &= h_{uk}^{lm(\text{even})}(t, r) e^{im\phi} Y_{lm}(\theta), \\ h_{uk}^{lm(\text{odd})}(t, r, \theta, \phi) &= h_{uk}^{lm(\text{odd})}(t, r) e^{im\phi} Y'_{lm}(\theta), \end{aligned} \quad (\text{A28})$$

and

$$\begin{aligned} h_{uk}^{lm(\text{even})}(t, r) &= u^t \left[ f(r)H_0^{lm}(t, r) + 2H_1^{lm}(t, r) \left( \frac{dr_0}{dt} \right) + f(r)^{-1}H_2^{lm}(t, r) \left( \frac{dr_0}{dt} \right)^2 + r^2 K^{lm}(t, r) \left( \frac{d\phi_0}{dt} \right)^2 \right], \\ h_{uk}^{lm(\text{odd})}(t, r) &= 2u^t \left( \frac{d\phi_0}{dt} \right) \left[ h_0^{lm}(t, r) + h_1^{lm}(t, r) \left( \frac{dr_0}{dt} \right)^2 \right]. \end{aligned} \quad (\text{A29})$$

Each of the even/odd time-domain RWZ metric perturbations,  $H_0^{lm}(t, r), \dots$ , are given by Fourier integrals, say  $H_0^{lm}(t, r) = \int d\omega H_0^{lm\omega}(r) e^{-i\omega t}, \dots$ , where  $H_0^{lm\omega}(r), \dots$  are linear combinations of the RW solutions  $R_{lm\omega}^{(\text{even/odd})}(r)$  and of their first radial derivatives. Therefore, Fourier-transforming  $h_{uk}^{lm(\text{even/odd})}(t, r)$  leads to (formally)

$$h_{uk,\pm}^{lm\omega(\text{even/odd})}(r) = K_{R_{\text{up/in}(\text{even/odd})}}^{lm\omega}(r) R_{lm\omega,\pm}^{(\text{even/odd})}(r) + K_{R'_{\text{up/in}(\text{even/odd})}}^{lm\omega}(r) R'_{lm\omega,\pm}^{(\text{even/odd})}(r). \quad (\text{A30})$$

Consider, for instance, the even contribution to the left part, i.e.,  $h_{uk,-}^{lm\omega(\text{even})}(r)$ . First replace  $R_{lm\omega,-}^{(\text{even})}$  with  $R_{\text{in}}^{lm\omega}$  through Eqs. (A26), (A27) to obtain

$$\begin{aligned} h_{uk,-}^{lm\omega(\text{even})}(r) &= \sum_n \frac{Y_{lm}^* \left( \frac{\pi}{2} \right)}{W_{lm\omega}} \left[ J_{\text{up}(\text{even})}^{lm\omega,n}(r_0)\delta_n + \tilde{J}_{\text{up}(\text{even})}^{lm\omega,n}(r_0)\delta'_n \right] \left[ K_{R_{\text{in}(\text{even})}}^{lm\omega}(r) R_{\text{in}}^{lm\omega}(r) + K_{R'_{\text{in}(\text{even})}}^{lm\omega}(r) R'_{\text{in}}^{lm\omega}(r) \right] \\ &\equiv \sum_n Y_{lm}^* \left( \frac{\pi}{2} \right) \left\{ \left[ C_1^{lm\omega,n}(r)\delta_n + \tilde{C}_1^{lm\omega,n}(r)\delta'_n \right] Z_1^{lm\omega}(r) + \dots \right\}, \end{aligned} \quad (\text{A31})$$

where

$$\begin{aligned}
C_1^{lm\omega,n}(r) &= J_{R_{\text{up}}(\text{even})}^{lm\omega,n}(r_0) K_{R_{\text{in}}(\text{even})}^{lm\omega}(r), & C_2^{lm\omega,n}(r) &= J_{R'_{\text{up}}(\text{even})}^{lm\omega,n}(r_0) K_{R_{\text{in}}(\text{even})}^{lm\omega}(r), \\
C_3^{lm\omega,n}(r) &= J_{R_{\text{up}}(\text{even})}^{lm\omega,n}(r_0) K_{R'_{\text{in}}(\text{even})}^{lm\omega}(r), & C_4^{lm\omega,n}(r) &= J_{R'_{\text{up}}(\text{even})}^{lm\omega,n}(r_0) K_{R'_{\text{in}}(\text{even})}^{lm\omega}(r), \\
\tilde{C}_1^{lm\omega,n}(r) &= \tilde{J}_{R_{\text{up}}(\text{even})}^{lm\omega,n}(r_0) K_{R_{\text{in}}(\text{even})}^{lm\omega}(r), & \tilde{C}_2^{lm\omega,n}(r) &= \tilde{J}_{R'_{\text{up}}(\text{even})}^{lm\omega,n}(r_0) K_{R_{\text{in}}(\text{even})}^{lm\omega}(r), \\
\tilde{C}_3^{lm\omega,n}(r) &= \tilde{J}_{R_{\text{up}}(\text{even})}^{lm\omega,n}(r_0) K_{R'_{\text{in}}(\text{even})}^{lm\omega}(r), & \tilde{C}_4^{lm\omega,n}(r) &= \tilde{J}_{R'_{\text{up}}(\text{even})}^{lm\omega,n}(r_0) K_{R'_{\text{in}}(\text{even})}^{lm\omega}(r), \\
Z_1^{lm\omega}(r) &= R_{\text{in}}^{lm\omega}(r) R_{\text{up}}^{lm\omega}(r_0) W_{lm\omega}^{-1}, & Z_2^{lm\omega}(r) &= R_{\text{in}}^{lm\omega}(r) R'_{\text{up}}^{lm\omega}(r_0) W_{lm\omega}^{-1}, \\
Z_3^{lm\omega}(r) &= R'_{\text{in}}^{lm\omega}(r) R_{\text{up}}^{lm\omega}(r_0) W_{lm\omega}^{-1}, & Z_4^{lm\omega}(r) &= R'_{\text{in}}^{lm\omega}(r) R'_{\text{up}}^{lm\omega}(r_0) W_{lm\omega}^{-1}.
\end{aligned} \tag{A32}$$

Properly transforming terms according to

$$f(\omega)\delta_n = f(\omega_{m,n})\delta_n, \quad f(\omega)\delta'_n = -f'(\omega_{m,n})\delta_n + f(\omega_{m,n})\delta'_n, \tag{A33}$$

and Fourier anti-transforming

$$h_{uk,-}^{lm(\text{even})}(t,r) = \frac{1}{2\pi} \int e^{-i\omega t} h_{uk,-}^{lm\omega(\text{even})}(r) d\omega, \tag{A34}$$

then yields

$$\begin{aligned}
h_{uk,-}^{(\text{even})}(t) &= \frac{1}{2\pi} \sum_{lmn} \left| Y_{lm} \left( \frac{\pi}{2} \right) \right|^2 e^{i(m\phi_0(t) - \omega_{m,n}t)} \left\{ \left[ \left( C_1^{lm,n} + it\tilde{C}_1^{lm,n} - \frac{d\tilde{C}_1^{lm\omega,n}}{d\omega} \Big|_{\omega=\omega_{m,n}} \right) Z_1^{lm,n} \right. \right. \\
&\quad \left. \left. - \tilde{C}_1^{lm,n} \frac{dZ_1^{lm\omega}}{d\omega} \Big|_{\omega=\omega_{m,n}} \right]_{r=r_0(t)} + \dots \right\},
\end{aligned} \tag{A35}$$

where all quantities are evaluated at the particle position  $r = r_0(t)$ . A similar procedure applies to the odd case.

The resulting  $h_{uk}(t)$  has to be averaged over a (coordinate-time) radial period, and once inserted in Eq. (A4) finally gives  $\delta U$ . The latter should be suitably regularized in order to remove its singular part. Barack and Sago [32] provided a closed form expression (in terms of elliptic integrals) for the regularization parameter  $B_H$  of the quantity  $H = \frac{1}{2}h_{uu}$  (see their Eq. (D15)), which is still a function of time, being evaluated at the particle position. A feature of our formalism is that, in order to compute the *regularized* value of  $\langle h_{uk} \rangle_t$ , we do not need to analytically determine in advance the corresponding subtraction term, because we automatically obtain it as a side-product of our computation [by taking the  $l \rightarrow \infty$  limit of our PN-based calculation.] The subtraction term (a.k.a. ‘‘regularization parameter’’) for the quantity  $U_0 \langle h_{uk} \rangle_t = \langle h_{uu} \rangle_\tau$  is

$$\begin{aligned}
B &= 2u_p - \frac{1}{2}u_p^2 - \frac{39}{32}u_p^3 - \frac{385}{128}u_p^4 - \frac{61559}{8192}u_p^5 - \frac{622545}{32768}u_p^6 - \frac{25472511}{524288}u_p^7 - \frac{263402721}{2097152}u_p^8 - \frac{176103411255}{536870912}u_p^9 \\
&+ \left( -2u_p + \frac{7}{4}u_p^2 + 7u_p^3 + \frac{8597}{256}u_p^4 + \frac{1498513}{8192}u_p^5 + \frac{69481763}{65536}u_p^6 + \frac{1650414477}{262144}u_p^7 + \frac{158088550401}{4194304}u_p^8 \right. \\
&\quad \left. + \frac{121418022556683}{536870912}u_p^9 \right) e^2 \\
&+ \left( -\frac{23}{16}u_p^2 - \frac{1655}{256}u_p^3 - \frac{16549}{512}u_p^4 - \frac{5554769}{32768}u_p^5 - \frac{229907593}{262144}u_p^6 - \frac{17904332713}{4194304}u_p^7 - \frac{77183281089}{4194304}u_p^8 \right. \\
&\quad \left. - \frac{63794507176773}{1073741824}u_p^9 \right) e^4 + O(u_p^{10}, e^6).
\end{aligned} \tag{A36}$$

It is simply related to that for  $\delta U$  by  $B_{\delta U} = \frac{1}{2}U_0 B$ . We checked that our (PN- and eccentricity-expanded) result for  $B$  agrees with the correspondingly-expanded (time-averaged) analytical result derived in [32], via  $B = 2\langle B_H \rangle_\tau$ .

The low multipoles ( $l = 0, 1$ ) have been computed separately (using the method of [16]). Their (already regularized) contribution to  $\delta U$  is the following



$$\begin{aligned}
\delta U^{l=0,1} = & -u_p - \frac{1}{2}u_p^2 - \frac{57}{32}u_p^3 - \frac{1325}{128}u_p^4 - \frac{417289}{8192}u_p^5 - \frac{7203141}{32768}u_p^6 - \frac{457801857}{524288}u_p^7 - \frac{6888106557}{2097152}u_p^8 \\
& - \frac{6386307327945}{536870912}u_p^9 \\
& + \left( u_p + \frac{9}{4}u_p^2 + \frac{7}{8}u_p^3 - \frac{7473}{256}u_p^4 - \frac{2080289}{8192}u_p^5 - \frac{108723171}{65536}u_p^6 - \frac{2615543903}{262144}u_p^7 - \frac{245438383189}{4194304}u_p^8 \right. \\
& \left. - \frac{183533858669131}{536870912}u_p^9 \right) e^2 \\
& + \left( -\frac{33}{16}u_p^2 + \frac{895}{256}u_p^3 + \frac{18815}{256}u_p^4 + \frac{16321729}{32768}u_p^5 + \frac{678595077}{262144}u_p^6 + \frac{49395616017}{4194304}u_p^7 + \frac{401066889193}{8388608}u_p^8 \right. \\
& \left. + \frac{171799575733669}{1073741824}u_p^9 \right) e^4 + O(u_p^{10}, e^6). \tag{A37}
\end{aligned}$$

**Appendix B: Coefficients of the PN expansions of the functions  $a(u_3)$ ,  $\bar{d}(u_3)$ ,  $\rho(u_3)$ , and  $q(u_3)$  (where  $u_3 \equiv 3u$ ).**

We list below in Tables VI, VII, VIII and IX the coefficients of the PN expansions of the functions  $a(u_3)$ ,  $\rho(u_3)$ ,  $\bar{d}(u_3)$  and  $q(u_3)$ , respectively, where  $u_3 \equiv 3u$ . For instance, the PN expansion of the EOB radial potential  $a(u)$  in powers of  $u_3$  is defined by Eq. (14), and similarly for the other EOB functions.

TABLE VI. Coefficients of the PN expansion of  $a(u_3)$  (where  $u_3 \equiv 3u$ ).

$N$	$\hat{a}_N$	$\hat{a}'_N$	$\hat{a}''_N$	$\hat{a}'''_N$	$\hat{a}''''_N$
3	$0.7407407407 \times 10^{-1}$	0	0	0	0
4	0.2307148148	0	0	0	0
5	$0.3885272716 \times 10^{-1}$	$0.5267489711 \times 10^{-1}$	0	0	0
6	$-0.8338706215 \times 10^{-1}$	$-0.9150172836 \times 10^{-1}$	0	0	0
7	0.3407031724	$-0.2847361682 \times 10^{-2}$	0	0	0
8	0.1039436274	0.1598400803	$-0.7952324342 \times 10^{-2}$	0	0
9	-0.4718506679	$-0.8953034274 \times 10^{-1}$	$0.1255096276 \times 10^{-1}$	0	0
10	0.2384172903	-0.1456465064	$0.3027617741 \times 10^{-2}$	0	0
11	0.6581815598	0.1243999564	$-0.2520471365 \times 10^{-1}$	$0.8003748299 \times 10^{-3}$	0
12	-0.4387682766	0.1582428946	$0.8613195585 \times 10^{-2}$	$-0.1083217892 \times 10^{-2}$	0
13	-0.4889356138	-0.1260270367	$0.2542670993 \times 10^{-1}$	$-0.6009925216 \times 10^{-3}$	0
14	0.5006006303	-0.1885956666	$-0.1182152359 \times 10^{-1}$	$0.2474966882 \times 10^{-2}$	$-0.6041644844 \times 10^{-4}$
15	0.5018616919	0.1112996214	$-0.2899966966 \times 10^{-1}$	$-0.706112373 \times 10^{-4}$	$0.6307853274 \times 10^{-4}$
16	-0.1446511265	0.2496830421	$0.995357387 \times 10^{-3}$	$-0.2455369950 \times 10^{-2}$	$0.6726163302 \times 10^{-4}$
17	-0.6989207457	$-0.2953308384 \times 10^{-1}$	$0.3736873206 \times 10^{-1}$	$-0.3176428511 \times 10^{-3}$	$-0.1602661295 \times 10^{-3}$
18	-0.2814052401	-0.3589800307	$0.1913120432 \times 10^{-1}$	$0.2652093198 \times 10^{-2}$	$-0.7390733724 \times 10^{-4}$
19	1.382632670	-0.1428658618	$-0.5474406082 \times 10^{-1}$	$0.3892284877 \times 10^{-2}$	$0.8759119256 \times 10^{-4}$
20	0.8449305382	0.5415180408	$-0.6363323976 \times 10^{-1}$	$-0.2718419238 \times 10^{-2}$	$0.1900895693 \times 10^{-3}$
21	-2.254005320	0.4263215985	$0.7445208813 \times 10^{-1}$	$-0.9823954351 \times 10^{-2}$	$0.3111490819 \times 10^{-4}$
22	-1.459428785	-0.8106346246	0.1510854162	$0.2828816180 \times 10^{-2}$	$-0.8152502117 \times 10^{-3}$
23	3.312652006	-0.9193948736	$-0.9370003950 \times 10^{-1}$	$0.2168105861 \times 10^{-1}$	$-0.4310759893 \times 10^{-3}$

**Acknowledgments**

We thank Maarten van de Meent for informative email exchanges about the precession function  $\rho(u)$ . D.B.

thanks the Italian INFN (Naples) for partial support and IHES for hospitality during the development of this project. All the authors are grateful to ICRA Net for partial support.

TABLE VII.  $(N - 1)^2$ -rescaled coefficients of the PN expansion of  $\rho(u_3)$ .

$N$	$\widehat{\rho}_N/(N - 1)^2$	$\widetilde{\rho}_N/(N - 1)^2$	$\widetilde{\rho}'_N/(N - 1)^2$
2	1.555555556	0	0
3	1.135439039	0	0
4	-0.163704216	0.229721079	0
5	-0.735645815	-0.416519694	0
6	1.349760034	0.104713538	0
7	-0.126387674	0.583029222	$-0.273913594 \times 10^{-1}$
8	-2.325715312	-0.676167975	$0.646912737 \times 10^{-1}$
9	2.513342107	-0.231444902	$-0.312270551 \times 10^{-1}$

TABLE VIII.  $(N - 1)^2$ -rescaled coefficients of the PN expansion of  $\bar{d}(u_3)$ .

$N$	$\widehat{d}_N/(N - 1)^2$	$\widetilde{d}_N/(N - 1)^2$	$\widetilde{d}'_N/(N - 1)^2$
2	0.666666667	0	0
3	0.481481481	0	0
4	0.244462862	$0.541380887 \times 10^{-1}$	0
5	$-0.6597928 \times 10^{-1}$	$-0.521751911 \times 10^{-1}$	0
6	0.299039195	$-0.390769700 \times 10^{-1}$	0
7	0.270278611	0.163046626	$-0.883592239 \times 10^{-2}$
8	-0.696093391	-0.103547802	$0.164167717 \times 10^{-1}$
9	0.531333085	-0.165934019	$-0.316508395 \times 10^{-3}$

- [1] A. Buonanno and T. Damour, “Effective one-body approach to general relativistic two-body dynamics,” *Phys. Rev. D* **59**, 084006 (1999) [gr-qc/9811091].
- [2] A. Buonanno and T. Damour, “Transition from inspiral to plunge in binary black hole coalescences,” *Phys. Rev. D* **62**, 064015 (2000) [gr-qc/0001013].
- [3] T. Damour, P. Jaranowski and G. Schaefer, “On the determination of the last stable orbit for circular general relativistic binaries at the third post-Newtonian approximation,” *Phys. Rev. D* **62**, 084011 (2000) [gr-qc/0005034].
- [4] T. Damour, “Coalescence of two spinning black holes: an effective one-body approach,” *Phys. Rev. D* **64**, 124013 (2001) [gr-qc/0103018].
- [5] A. Le Tiec, L. Blanchet and B. F. Whiting, “The First Law of Binary Black Hole Mechanics in General Relativity and Post-Newtonian Theory,” *Phys. Rev. D* **85**, 064039 (2012) [arXiv:1111.5378 [gr-qc]].
- [6] L. Blanchet, A. Buonanno and A. Le Tiec, “First law of mechanics for black hole binaries with spins,” *Phys. Rev. D* **87**, no. 2, 024030 (2013) [arXiv:1211.1060 [gr-qc]].
- [7] A. Le Tiec, “First Law of Mechanics for Compact Binaries on Eccentric Orbits,” *Phys. Rev. D* **92**, no. 8, 084021 (2015) [arXiv:1506.05648 [gr-qc]].
- [8] T. Damour, “Gravitational Self Force in a Schwarzschild Background and the Effective One Body Formalism,” *Phys. Rev. D* **81**, 024017 (2010) [arXiv:0910.5533 [gr-qc]].
- [9] L. Barack, T. Damour and N. Sago, “Precession effect of the gravitational self-force in a Schwarzschild spacetime and the effective one-body formalism,” *Phys. Rev. D* **82**, 084036 (2010) [arXiv:1008.0935 [gr-qc]].
- [10] A. Le Tiec, E. Barausse and A. Buonanno, “Gravitational Self-Force Correction to the Binding Energy of Compact Binary Systems,” *Phys. Rev. Lett.* **108**, 131103 (2012) [arXiv:1111.5609 [gr-qc]].
- [11] E. Barausse, A. Buonanno and A. Le Tiec, “The complete non-spinning effective-one-body metric at linear order in the mass ratio,” *Phys. Rev. D* **85**, 064010 (2012) [arXiv:1111.5610 [gr-qc]].
- [12] S. Akcay, L. Barack, T. Damour and N. Sago, “Gravitational self-force and the effective-one-body formalism between the innermost stable circular orbit and the light ring,” *Phys. Rev. D* **86**, 104041 (2012) [arXiv:1209.0964 [gr-qc]].
- [13] A. G. Shah, J. L. Friedman and B. F. Whiting, “Finding high-order analytic post-Newtonian parameters from a high-precision numerical self-force calculation,” *Phys. Rev. D* **89**, no. 6, 064042 (2014) [arXiv:1312.1952 [gr-qc]].
- [14] D. Bini and T. Damour, “High-order post-Newtonian contributions to the two-body gravitational interaction potential from analytical gravitational self-force calculations,” *Phys. Rev. D* **89**, no. 6, 064063 (2014) [arXiv:1312.2503 [gr-qc]].
- [15] S. R. Dolan, N. Warburton, A. I. Harte, A. Le Tiec, B. Wardell and L. Barack, “Gravitational self-torque and spin precession in compact binaries,” *Phys. Rev. D* **89**, no. 6, 064011 (2014) [arXiv:1312.0775 [gr-qc]].

TABLE IX.  $(N - 1)^4$ -rescaled coefficients of the PN expansion of  $q(u_3)$ .

$N$	$\hat{q}_N/(N - 1)^4$	$\tilde{q}'_N/(N - 1)^4$	$\tilde{q}''_N/(N - 1)^4$
2	0.888888889	0	0
3	$0.664607507 \times 10^{-1}$	0	0
4	$-0.234627665 \times 10^{-1}$	$0.787917057 \times 10^{-2}$	0
5	$0.155706161 \times 10^{-1}$	$-0.157616639 \times 10^{-1}$	0
6	$0.683824536 \times 10^{-1}$	$0.327993634 \times 10^{-1}$	$-0.141710523 \times 10^{-2}$
7	-0.221679525	$-0.332538735 \times 10^{-1}$	$0.405402116 \times 10^{-2}$
8	0.262385007	$-0.296664893 \times 10^{-1}$	$-0.274350852 \times 10^{-2}$

- [16] T. S. Keidl, A. G. Shah, J. L. Friedman, D. H. Kim and L. R. Price, “Gravitational Self-force in a Radiation Gauge,” Phys. Rev. D **82**, no. 12, 124012 (2010) [Phys. Rev. D **90**, no. 10, 109902 (2014)] [arXiv:1004.2276 [gr-qc]].
- [17] A. G. Shah, J. L. Friedman and T. S. Keidl, “EMRI corrections to the angular velocity and redshift factor of a mass in circular orbit about a Kerr black hole,” Phys. Rev. D **86**, 084059 (2012) [arXiv:1207.5595 [gr-qc]].
- [18] D. Bini and T. Damour, “Analytical determination of the two-body gravitational interaction potential at the fourth post-Newtonian approximation,” Phys. Rev. D **87**, no. 12, 121501 (2013) [arXiv:1305.4884 [gr-qc]].
- [19] D. Bini and T. Damour, “Two-body gravitational spin-orbit interaction at linear order in the mass ratio,” Phys. Rev. D **90**, no. 2, 024039 (2014) [arXiv:1404.2747 [gr-qc]].
- [20] S. R. Dolan, P. Nolan, A. C. Ottewill, N. Warburton and B. Wardell, “Tidal invariants for compact binaries on quasicircular orbits,” Phys. Rev. D **91**, no. 2, 023009 (2015) [arXiv:1406.4890 [gr-qc]].
- [21] D. Bini and T. Damour, “Gravitational self-force corrections to two-body tidal interactions and the effective one-body formalism,” Phys. Rev. D **90**, no. 12, 124037 (2014) [arXiv:1409.6933 [gr-qc]].
- [22] D. Bini and T. Damour, “Detweiler’s gauge-invariant redshift variable: Analytic determination of the nine and nine-and-a-half post-Newtonian self-force contributions,” Phys. Rev. D **91**, 064050 (2015) [arXiv:1502.02450 [gr-qc]].
- [23] D. Bini and T. Damour, “Analytic determination of high-order post-Newtonian self-force contributions to gravitational spin precession,” Phys. Rev. D **91**, no. 6, 064064 (2015) [arXiv:1503.01272 [gr-qc]].
- [24] S. Akcay, A. Le Tiec, L. Barack, N. Sago and N. Warburton, “Comparison Between Self-Force and Post-Newtonian Dynamics: Beyond Circular Orbits,” Phys. Rev. D **91**, no. 12, 124014 (2015) [arXiv:1503.01374 [gr-qc]].
- [25] C. Kavanagh, A. C. Ottewill and B. Wardell, “Analytical high-order post-Newtonian expansions for extreme mass ratio binaries,” Phys. Rev. D **92**, no. 8, 084025 (2015) [arXiv:1503.02334 [gr-qc]].
- [26] M. van de Meent and A. G. Shah, “Metric perturbations produced by eccentric equatorial orbits around a Kerr black hole,” Phys. Rev. D **92**, no. 6, 064025 (2015) [arXiv:1506.04755 [gr-qc]].
- [27] D. Bini, T. Damour and A. Geralico, “Confirming and improving post-Newtonian and effective-one-body results from self-force computations along eccentric orbits around a Schwarzschild black hole,” Phys. Rev. D **93**, no. 6, 064023 (2016) [arXiv:1511.04533 [gr-qc]].
- [28] S. Hopper, C. Kavanagh and A. C. Ottewill, “Analytic self-force calculations in the post-Newtonian regime: eccentric orbits on a Schwarzschild background,” Phys. Rev. D **93**, no. 4, 044010 (2016) [arXiv:1512.01556 [gr-qc]].
- [29] S. Akcay and M. van de Meent, “Numerical computation of the effective-one-body potential  $q$  using self-force results,” Phys. Rev. D **93**, no. 6, 064063 (2016) [arXiv:1512.03392 [gr-qc]].
- [30] A. G. Shah and A. Pound, “Linear-in-mass-ratio contribution to spin precession and tidal invariants in Schwarzschild spacetime at very high post-Newtonian order,” Phys. Rev. D **91**, no. 12, 124022 (2015) [arXiv:1503.02414 [gr-qc]].
- [31] S. L. Detweiler, “A Consequence of the gravitational self-force for circular orbits of the Schwarzschild geometry,” Phys. Rev. D **77**, 124026 (2008) [arXiv:0804.3529 [gr-qc]].
- [32] L. Barack and N. Sago, “Beyond the geodesic approximation: conservative effects of the gravitational self-force in eccentric orbits around a Schwarzschild black hole,” Phys. Rev. D **83**, 084023 (2011) [arXiv:1101.3331 [gr-qc]].
- [33] T. Damour, P. Jaranowski and G. Schäfer, “Fourth post-Newtonian effective one-body dynamics,” Phys. Rev. D **91**, no. 8, 084024 (2015) [arXiv:1502.07245 [gr-qc]].
- [34] S. Mano, H. Suzuki and E. Takasugi, “Analytic solutions of the Regge-Wheeler equation and the post-Minkowskian expansion,” Prog. Theor. Phys. **96**, 549 (1996) [gr-qc/9605057].
- [35] S. Mano, H. Suzuki and E. Takasugi, “Analytic solutions of the Teukolsky equation and their low frequency expansions,” Prog. Theor. Phys. **95**, 1079 (1996) [gr-qc/9603020].
- [36] L. Blanchet, S. L. Detweiler, A. Le Tiec and B. F. Whiting, “High-Order Post-Newtonian Fit of the Gravitational Self-Force for Circular Orbits in the Schwarzschild Geometry,” Phys. Rev. D **81**, 084033 (2010) [arXiv:1002.0726 [gr-qc]].
- [37] L. Blanchet, G. Faye and B. F. Whiting, “Half-integral conservative post-Newtonian approximations in the redshift factor of black hole binaries,” Phys. Rev. D **89**, no. 6, 064026 (2014) [arXiv:1312.2975 [gr-qc]].
- [38] M. van de Meent et al., in preparation
- [39] L. Blanchet and T. Damour, “Tail Transported Temporal Correlations in the Dynamics of a Gravitating System,” Phys. Rev. D **37**, 1410 (1988).

- [40] T. Damour, P. Jaranowski and G. Schäfer, “Nonlocal-in-time action for the fourth post-Newtonian conservative dynamics of two-body systems,” *Phys. Rev. D* **89**, no. 6, 064058 (2014) [arXiv:1401.4548 [gr-qc]].